EFFECT OF TIME-DEPENDENT TRANSPIRATION ON AXISYMMETRIC STAGNATION-POINT FLOW AND HEATTRANSFER OF A VISCOUS FLUID ON A MOVING CIRCULAR CYLINDER

B. Haghighi
Ferdowsi University of Mashhad, P.O. Box No. 91775-1111, Mashhad, Iran

A. B. Rahimi*
Ferdowsi University of Mashhad, P. O. Box No. 91775-111, Mashhad, Iran
rahimiab@yahoo.com

*Corresponding Author.

(Received: July 9, 2009 – Accepted in Revised Form: March 11, 2010)

Abstract Effect of time dependent normal transpiration $U_0(t)$ on the problem of unsteady viscous flow and heat transfer in the vicinity of an axisymmetric stagnation point of an infinite circular cylinder moving simultaneously with time-depended angular and axial velocities and with time-dependent wall temperature or wall heat flux are investigated. The impinging free stream is steady with a strain rate $\bar{k}$. A reduction of Navier-Stokes equations and energy equation is obtained by use of appropriate transformations. The general semi-similar solutions are obtained when angular and axial velocities of the cylinder and also its wall temperature or its wall heat flux vary as certain functions of time. The cylinder may perform different types of motions. It may move or rotate with constant speed, with exponentially increasing/decreasing axial/angular velocity, with harmonically varying axial/angular speed, or with accelerating/decelerating oscillatory axial/angular speed. The cylinder surface temperature or its surface heat flux may have the same type of behavior as the cylinder motion. Semi-similar solutions of the unsteady Navier-Stokes and energy equations are obtained numerically using a finite-difference scheme. All the solutions above are presented for different Reynolds numbers ($\mathrm{Re} = \bar{k}a^2/2u$) and different functions of dimensionless transpiration rate, $S(t) = U_0(t)/(\bar{k}a)$, where a is cylinder radius and ν is kinematic viscosity of the fluid. Shear stresses corresponding to all the cases increase with the increase of Reynolds number and decrease with the increase of suction rate. The maximum value of shear stress increases with increase of oscillation frequency and amplitude. An interesting result is obtained in which a cylinder moving with certain angular/axial velocity function and at particular values of Reynolds number is azimuthally/axially stress-free. Heat transfer rate increases with the increase of the rate of suction, Reynolds number, and Prandtl number. Interesting means of heating and cooling processes of cylinder surface are obtained using different rate of transpiration.

Keywords Stagnation-point Flow, Time-dependent Axial/Angular Velocity, Time Dependent Heat Transfer, Time Dependent Transpiration, Semi-similar Solution, Finite Difference Method.

چکیده اثر مکش و دمش عمودی تابع زمان در مساله جریان لزج نا پایدارو انتقال حرارت در ناحیه یک نقطه سکون متقارن بر روی یک سیلندر طویل با سطح مقطع دایروی که به طور هم‌زمان دارای چرخش با سرعت زاویه‌ای تابع زمان و همچنین سرعت محوری تابع زمان می‌باشد و نیز درجه حرارت دیوار و یا شار حرارتی دیواره تابعی از زمان می‌باشد مورد بررسی قرار می‌گیرد. سیال برخورد کننده پایدار و با قدرت معینی می باشد. یک چنین مکانیزم های با مکش و دمش تابع زمان در سیستم‌های اسپری در صنایع غذایی، در تزریق سوخت و غیره کاربرد فراوان دارند. این سیلندر دارای حرکات مختلفی می‌تواند باشد که شامل موارد ذیل می‌باشند: حرکت محوری و دورانی با سرعت ثابت، حرکت با سرعت تابع نمایی افزایشی یا کاهشی به صورت محوری و دورانی، حرکت محوری و دورانی هارمونیک متغیر، و یا حرکت نوسانی افزایشی و یا کاهشی. درجه حرارت سطح این سیلندر و یا شار حرارتی سطح این سیلندر می‌تواند به صورت توابع یکسانی با سرعت آن باشد. حل‌های نیمه تشابهی معادلات ناپایدار ناویه-استوکس و انرژی به صورت عددی و با استفاده از روش‌های تفاضل محدود به دست آورده می‌شوند. این نتایج برای مقادیر مختلفی از عدد رینولدز و توابع متفاوتی از نرخ مکش و دمش ارائه می‌شوند. تنش‌های برشی مرتبط با همه موارد با افزایش عدد رینولدز افزایش و با افزایش نرخ مکش و دمش کاهش می‌یابند. نرخ انتقال حرارت نیز با افزایش نرخ مکش و دمش، عدد رینولدز، و عدد پرانتل افزایش می‌یابد.

1. INTRODUCTION

The task of finding exact solution for Navier-Stokes equations is the difficult one due to nonlinearity of these equations. Hiemenz [1] has obtained exact solution of the Navier-Stokes equations governing the two-dimensional stagnation-point flow on a flat plate. The analogous axisymmetric stagnation-point flow was investigated by Homan [2]. Result of the problem of stagnation-point flow against the flat plate for axisymmetric cases were presented by Howarth [3] and Davey [4]. Wang [5] was first to find exact solution for the problem of axisymmetric stagnation flow on an infinite stationary circular cylinder. Gorla [6-10], in a series of papers, studied the steady and unsteady flows and heat transfer over a circular cylinder on the vicinity of the stagnation-point for the cases of constant axial movement, and then special case of axial harmonic motion of a nonrotating cylinder. This special case is only for small and high values of the frequency parameter using perturbation techniques. Cunning, Davis and Weidman [11] have considered the stagnation flow problem on a rotating circular cylinder with constant angular velocity, including the effects of suction and blowing with constant rate. Takhar, Chamkha and Nath [12], have also investigated the unsteady viscous flow in the vicinity of an axisymmetric stagnation point of an infinite circular cylinder when both the cylinder and the free-stream velocities vary as the same function of time. Their self-similar solution is only for the case when both the cylinder and the free-stream velocities vary inversely as a linear function of time and by taking an average value for the Reynolds number. The study considered by Rahimi [13] presents a systematic solution of Gorla's results for high Prandtl number fluids using an inner-outer expansion of fluid properties. Recently, Saleh and Rahimi [14-19] have investigated the unsteady viscous flow and heat transfer in the vicinity of an axisymmetric stagnation point of an infinite rotating and moving circular cylinder with time-dependent angular and axial velocity and time-dependent wall temperature or wall heat flux with uniform normal transpiration. The effect of time-dependent normal transpiration, the cylinder movement /rotation with time-dependent axial /angular velocity and time-dependent heat transfer, which are of interest in certain manufacturing processes, have not yet been considered. In the present analyses, the unsteady viscous flow and heat transfer in the vicinity of axisymmetric stagnation point of an infinite circular cylinder with time-dependent axial movement /rotation with time-dependent transpiration considered, though the reduction of Navier-Stokes equations and energy equation is obtained for the most general case of time-dependent transpiration rate. Our motivation is to generalize the problem of stagnation-point flow and heat transfer of a fluid on a moving /rotating cylinder. An exact solution of Navier-Stokes equation and energy equation is obtained. The general semi-similar solution is obtained when the axial /angular velocity of the cylinder and its surface temperature or heat flux vary in a prescribed manner. The cylinder may perform different types of motion / rotation. It may move with constant speed, with exponentially increasing- decreasing axial/angular velocity, with harmonically varying axial/angular speed, or with accelerating-decelerating oscillatory axial/angular speed. The cylinder surface temperature or its surface heat flux may have the same behavior as the cylinder motion. Sample distribution of shear stresses and temperature fields at Reynolds number ranging from 0.1 to 100 are presented for different forms of cylinder movement and different values of Prandtl and selected values of uniform suction and blowing rates. Particular cases of these results compared with existing results of Wang [5] and Gorla [6, 7, 9, 10], Cunning, Davis and Weidman [11], correspondingly. For completeness semi-similar solution of Navier-Stokes equations and energy equation are obtained and results for various examples of cylinder motion are presented for different values of flow parameters.

2. PROBLEM FORMULATION

Flow is considered in cylindrical coordinates (r, j, z) with corresponding velocity components (u, v, w), see Fig.1. We consider the laminar unsteady incompressible flow and heat transfer of a viscous fluid of a neighborhood of an axisymmetric stagnation point of an infinite circular cylinder when move axially or rotate with

a velocity variation with respect to time. An external axisymmetric radial stagnation flow of strain rate $\bar{k}$ impinges on the cylinder of radius a centered at $r = 0$. Time-dependent normal transpiration $U_0(t)$ at the cylinder surface may occur, where $U_0(t) > 0$ correspond to suction into the cylinder, though the formulation of the problem is for the more general case of time-dependent transpiration rate. The unsteady Navier-Stokes and energy equations in cylindrical polar coordinates governing the axisymmetric flow and heat transfer are given [5-10]:

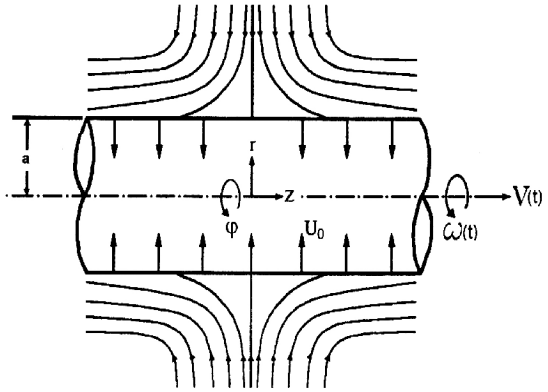

Figure 1. Schematic diagram of an axially moving and rotating cylinder under radial stagnation flow in the fixed cylindrical coordinate system (r, j, z)

Mass:

$$\frac{\partial}{\partial r}(ru) + r\frac{\partial w}{\partial z} = 0 \tag{1}$$

Mommentum:

$$\frac{\partial u}{\partial t} + u\frac{\partial u}{\partial r} - \frac{v^2}{r} = -\frac{1}{r}\frac{\partial p}{\partial r} + u\left(\frac{\partial^2 u}{\partial r^2} + \frac{1}{r}\frac{\partial u}{\partial r} - \frac{u}{r^2}\right) \tag{2}$$

$$\frac{\partial v}{\partial t} + u\frac{\partial v}{\partial r} - \frac{uv}{r} = u\left(\frac{\partial^2 v}{\partial r^2} + \frac{1}{r}\frac{\partial v}{\partial r} - \frac{v}{r^2}\right) \tag{3}$$

$$\frac{\partial w}{\partial t} + u\frac{\partial w}{\partial r} + w\frac{\partial w}{\partial z} = -\frac{1}{r}\frac{\partial p}{\partial z} + u\left(\frac{\partial^2 w}{\partial r^2} + \frac{1}{r}\frac{\partial w}{\partial r}\right) \tag{4}$$

Energy:

$$\frac{\partial T}{\partial t} + u\frac{\partial T}{\partial r} = a\left(\frac{\partial^2 T}{\partial r^2} + \frac{1}{r}\frac{\partial T}{\partial r}\right) \tag{5}$$

Where p, r, u and $\bar{a}$ are the fluid pressure, density kinematic viscosity, thermal diffusivity the boundary condition for velocity fields are:

$$r = a:\ u = -U_0(t),\ v = aw(t), w = V(t) \tag{6}$$

$$r \to \infty:\ \frac{\partial u}{\partial r} = -\bar{k},\ \lim_{r\to\infty} rv = 0,\ w = 2\bar{k}z \tag{7}$$

in which, (6) are no-slip conditions on the cylinder wall. Relation (7) shows that the viscous flow solution approaches, in a manner analogous to the Hiemenz flow, the potential flow solution as $r \to \infty$ [11].

For the temperature field we have:

$$\begin{aligned} &r = a: i)\ T = T_W(t)\ \ for defined wall temperature \\ &\quad ii)\ \frac{\partial T}{\partial r} = -\frac{q_W(t)}{k}\ \ for defined wall heat flux \\ &r \to \infty: T \to T_\infty \end{aligned} \tag{8}$$

where k is thermal conductivity of fluid and $T_W(t)$ and $q_W(t)$ are temperature and heat flux at the wall cylinder, respectively.

A reduction of the Navier-Stokes equations is obtained by the following coordinate separation of the velocity field [14, 15]:

$$u = -\bar{k}\frac{a}{\sqrt{h}}F(h,t),\ v = \frac{a}{\sqrt{h}}G(h,t)$$
$$w = 2\bar{k}F'(h,t)z + H(h,t),\ p = r\bar{k}^2a^2P \tag{9}$$

where $t = 2\bar{k}t$ and $h = (\frac{r}{a})^2$ are dimensionless time and radial variables and prime denotes differentiation with respect to h. Transformations (9) satisfy (1) automatically and insertion into (2), (3) and (4) yields a coupled system of differential equation in term of $F(h,t)$, $G(h,t)$ and $H(h,t)$ an expression for the pressure:

$$hF''' + F'' + \mathrm{Re}[1-(F')^2 + FF'' - \frac{\partial F'}{\partial t}] = 0 \qquad (10)$$

$$hG'' + \mathrm{Re}[FG' - \frac{\partial G}{\partial t}] = 0 \qquad (11)$$

$$hH'' + H' + \mathrm{Re}[FH' - F'H - \frac{\partial H}{\partial t}] = 0 \qquad (12)$$

$$P - P_0 = -[\frac{F^2}{2h} + \frac{1}{\mathrm{Re}}F' + 2(\frac{z}{a})^2 - \frac{1}{2\bar{k}^2}\int_1^h \frac{G^2(z)}{z^2}dz\,] \qquad (13)$$

In these equations prime denotes differentiation with respect to h and $\mathrm{Re} = \frac{\bar{k}a^2}{2n}$ is the Reynolds number.

From conditions (6) and (7), the boundary conditions for (10), (11) and (13) are as follows:

$$\begin{aligned} &h=1 : F = S(t), \quad F' = 0, \quad G = w(t), \quad H = V(t) \\ &h \to \infty: \quad F' = 1, \quad G = 0, \quad H = 0 \end{aligned} \qquad (14)$$

in which, $S(t) = \frac{U_0(t)}{\bar{k}a}$ is the dimensionless wall transpiration rate. To transform the energy equation into a non-dimensional form for the case of defined wall temperature, we introduce

$$\Theta = \frac{T(h,t) - T_\infty}{T_w(t) - T_\infty} \qquad (15)$$

Making use of (9) and (15), the energy equation may be
Written as:

$$h\Theta'' + \Theta' + \mathrm{Re}.\mathrm{Pr}(F\Theta' - \frac{\partial \Theta}{\partial t} - \frac{\frac{dT_w}{dt}}{T_w - T_\infty}) = 0 \qquad (16)$$

with the boundary condition as:

$$\Theta(1,t) = 1, \quad \Theta(\infty,t) = 0 \qquad (17)$$

For the case for defined wall heat flux, we introduce

$$\Theta = \frac{T(h,t) - T_\infty}{\frac{aq_w(t)}{2k}} \qquad (18)$$

Now, using equations (9) and (18), the energy equation may be written as:

$$h\Theta'' + \Theta' + \mathrm{Re}.\mathrm{Pr}(F\Theta' - \frac{\partial \Theta}{\partial t} - \frac{\frac{dq_w}{dt}}{q_w}) = 0 \qquad (19)$$

with the boundary condition as:

$$\Theta'(1,t) = -1, \quad \Theta(\infty,t) = 0 \qquad (20)$$

Here, equations (10), (11), (12), and (16) or (19) are for different forms of $S(t)$, $w(t)$, $V(t)$, $T_W(t)$ or $q_W(t)$ functions and were solved numerically with Re and Pr as parameters.

3. SELF-SIMILLAR EQUATIONS

There are time-dependent transpiration and also the term in equation (10) cannot be reduced to a system of ordinary differential equation, But; equations (11), (12), (16) and (19) can be reduced to a system of ordinary differential equation f. So, we assume that the function $G(h,t)$ in(11), $H(h,t)$ in(12) and $\Theta(h,t)$ in (16) and (19) are separable as:

$$G(h,t)=g(h).f(t)$$
$$H(h,t)=h(h).V(t) \quad (21)$$
$$\Theta(h,t)=q(h).Q(t)$$

Substituting these separation of variable into (11), (12), (16) and (19), correspondingly gives:

$$h\frac{g''}{g'}+\frac{g'}{g}+\mathrm{Re}\,F\frac{g'}{g}=\frac{\mathrm{Re}}{f(t)}.\frac{df(t)}{dt} \quad (22)$$

$$h\frac{h''}{h'}+\frac{h'}{h}+\mathrm{Re}(F\frac{h'}{h}-F')=\frac{\mathrm{Re}}{V(t)}.\frac{dV(t)}{dt} \quad (23)$$

for defined wall temperature:

$$h\frac{q''}{q}+\frac{q'}{q}+\mathrm{Re}.\mathrm{Pr}(\frac{Fq'}{q})=\mathrm{Re}.\mathrm{Pr}(\frac{\frac{dQ}{dt}}{Q}+\frac{\frac{dT_w}{dt}}{T_w-T_\infty}) \quad (24)$$

or for defined wall heat flux:

$$h\frac{q''}{q}+\frac{q'}{q}+\mathrm{Re}.\mathrm{Pr}(\frac{Fq'}{q})=\mathrm{Re}.\mathrm{Pr}(\frac{\frac{dQ}{dt}}{Q}+\frac{\frac{dq_w}{dt}}{q_w}) \quad (25)$$

The general solution to the differential equations (22), (23), (24) and (25), with t as an independent variable are as the following:

$$w(t)=b.Exp[(a+ib)t] \quad (26)$$

$$V(t)=b.Exp[(a+ib)t] \quad (27)$$

for defined wall temperature

$$Q(t)=\frac{c.Exp[(a+ib)t]}{T_w-T_\infty} \quad (28)$$

for defined wall heat flux

$$Q(t)=\frac{c.Exp[(a+ib)t]}{q_w(t)} \quad (29)$$

Here, $i=\sqrt{-1}$ and a , b , b and c are constants. Substituting these equation into the differential equations in (26), (27) and (28) or (29) with h as an independent variable results in:

$$hg''+\mathrm{Re}(Fg'-ag-ibg)=0 \quad (30)$$

$$hh''+h'+\mathrm{Re}(Fh'-Fh-ah-ibh)=0 \quad (31)$$

$$hq''+q'+\mathrm{Re}.\mathrm{Pr}(Fq'-aq-ibq)=0 \quad (32)$$

The angular velocity boundary conditions are:

$$G(1,t)=w(t)=g(1).f(t)\rightarrow g(1)=1 \quad (33)$$

$$G(\infty,t)=0=g(\infty).f(t)\rightarrow g(\infty)=0 \quad (34)$$

The axial velocity boundary conditions are:

$$H(1,t)=V(t)=h(1).V(t)\rightarrow h(1)=1 \quad (35)$$

$$H(\infty,t)=0=h(\infty).V(t)\rightarrow h(\infty)=0 \quad (36)$$

For the above defined wall temperature and wall heat flux, respectively, the result was obtained:

$$\Theta(1,t)=1=q(1).Q(t)$$
$$\Rightarrow\begin{cases}q(1)=1\\Q(t)=1\end{cases}\rightarrow T_w-T_\infty=c.Exp[(a+ib)t] \quad (37)$$

$$\Theta'(1,t)=-1=q'(1).Q(t)$$
$$\Rightarrow\begin{cases}q'(1)=-1\\Q(t)=1\end{cases}\rightarrow q_w(t)=c.Exp[(a+ib)t] \quad (38)$$

$$\Theta(\infty,t)=0=q(\infty).Q(t)\Rightarrow q(\infty)=0 \quad (39)$$

Note that in (26) $b=0$ correspond to the case of non-rotating cylinder, as presented by Wang [5]. If $b\neq 0$ and $a=b=0$, (26) gives the case of uniformly rotating cylinder with constant angular velocity, as given by Cunning et al. [11]. $b\neq 0, a\neq 0$ and $b=0$ correspond to the case of a pure harmonic rotation of cylinder. The case of

$a \neq 0, b \neq 0, b \neq 0$ is the most general which is considered in this paper. In (27) $b = 0$ corresponds to the case of cylinder with no axial movement, presented by Wang [5]. If $b \neq 0$ and $a = b = 0$, (27) gives the case of uniformly moving cylinder with constant axial velocity [7]. $b \neq 0, a \neq 0$ and $b = 0$ correspond to the case of a moving cylinder with harmonic velocity in its own plane, given by Gorla [9]. The case of $a \neq 0, b \neq 0, b \neq 0$ is the most general which is considered in this paper.

In (37) and (38) the cylinder surface temperature or its surface heat flux may have the same type of behavior as the cylinder motion. To obtain solution of equations (30), (31) and (32), it is assumed that the function $g(h)$, $h(h)$ and $q(h)$ are complex functions as:

$$g(h) = g_1(h) + ig_2(h) \tag{40}$$

$$h(h) = h_1(h) + ih_2(h) \tag{41}$$

$$q(h) = q_1(h) + iq_2(h) \tag{42}$$

Substituting (30), (31) and (32) into (30), (31) and (32), respectively, the following couple differential equations are obtained:

$$\begin{cases} hg_1'' + \mathrm{Re}(Fg_1' - ag_1 - ibg_2) = 0 \\ hg_2'' + \mathrm{Re}(Fg_2' - ag_2 - ibg_1) = 0 \end{cases} \tag{43}$$

$$\begin{cases} hh_1'' + h_1' + \mathrm{Re}(Fh_1' - F'h_1 - ah_1 - ibh_2) = 0 \\ hh_2'' + h_2' + \mathrm{Re}(Fh_2' - F'h_2 - ah_2 - ibh_1) = 0 \end{cases} \tag{44}$$

$$\begin{cases} hq_1'' + q_1' + \mathrm{Re}.\mathrm{Pr}(Fq_1' - aq_1 - ibq_2) = 0 \\ hq_2'' + q_2' + \mathrm{Re}.\mathrm{Pr}(Fq_2' - aq_2 - ibq_1) = 0 \end{cases} \tag{45}$$

The boundary conditions for functions F, G, H and Θ become:

$$h = 1 \ : \ F = S(t), F' = 0, g = 0, h = 1, q = 0 \quad (or\ q' = -1) \tag{46}$$

$$h \to \infty \ : F' = 0, g = 0, h = 0, q = 0 \tag{47}$$

where, $S(t) = \dfrac{U_0(t)}{\Gamma a}$ is the dimensionless wall transpiration rate which is time-dependent. Hence, the boundary condition sonfunctions h_1, h_2, g_1, g_2, q_1 and q_2 are:

$$h = 1 \ : \ F = S(t), F' = 0, g = 0, h = 1, q = 0 \quad (or\ q' = -1) \tag{48}$$

$$h \to \infty \ : F' = 0, g = 0, h = 0, q = 0 \tag{49}$$

The coupled system of equations (43), (44) and (45), along with boundary conditions (48) and (49), were solved using the forth-order Runge-Kutta method of numerical integration along with a shooting method as presente by Press et al.[13]. First, Eq. (9) was solved by guessing initial values for $F''(1)$ and integrating until the convergence reached. Then, the initial values of $h_1'(1)$, $h_2'(1)$, $g_1'(1)$, $g_2'(1)$ and $q_1'(1)$, $q_2'(1)$ [or $q_1(1)$, $q_2(1)$] were guessed and then integration was repeated until convergence was obtained. The value of $h_1(h)$, $h_2(h)$, $g_1(h)$, $g_2(h)$ and $q_1(h)$, $q_2(h)$ was assumed initially and then by repeating the integration of these three system of equations, final values were obtained.

4. SEMI-SIMILLAR EQUATIONS

Equations (9), (10), (11), (16) and (19) may be solved directly for every chosen $S(t)$, $w(t)$, $V(t)$, $T_W(t)$ or $q_W(t)$ functions. These obtained solutions are called semi-similar solution. These equations along with boundary conditions, (14), (17) and (20) were solved by using a central finite-difference method which lead to a tri-diagonal matrix. Assuming steady state for $t \leq 0$, the solution starts from $S(0), w(0), V(0), T_W(0)$ or $q_W(0)$ and marching through time, time-dependent solution for $t > 0$ were obtained. Sample axial and angular velocity profiles will be presented in later sections.

5. SHEAR STRESS

The shear stress at the cylinder surface is calculated from [11]:

$$s = m[r\frac{\partial}{\partial r}(\frac{n}{r})\hat{e}_j + \frac{\partial w}{\partial r}\hat{e}_z]_{r=a} \quad (50)$$

where, m is the fluid viscosity. Using definition (9), the shear stress at the cylinder surface for semi-similar solution becomes:

$$s = 2m[G'(1,t) - w(t)]\hat{e}_j + \frac{2m}{a}[2\Gamma F''(1,t)z + H'(1,t)]\hat{e}_z \quad (51)$$

Azimuthal surface shear stress for self-similar solutions is presented by the following relation:

$$\begin{aligned} s_j &= s_{j1} + is_{j2} \\ &= 2m\, b.Exp(at)\{[\cos(bt)(g'(1)-1) - \\ &\quad \sin(bt)g_2'(1)] + i[\sin(bt)(g'(1)-1) - \\ &\quad \cos(bt)g_2'(1)]\} \end{aligned} \quad (52)$$

Axial surface shear stress for self-similar solutions is presented by the following relation:

$$\begin{aligned} s_z &= s_{z1} + is_{z2} \\ &= \frac{2m}{a}\{2\Gamma F''(1,t)z + bExp(at)[(h'(1)\cos(bt) \\ &\quad - h_2'(1)\sin(bt)) + i(h'(1)\sin(bt) + \\ &\quad + h_2'(1)\cos(bt))]\} \end{aligned} \quad (53)$$

Some numerical values of real part of azimuthal and axial shear stress will be presented later for few examples of angular and axial velocities, respectively. Of course, it is noted that the real and imaginary parts of this quantity are actually the same but with a phase difference of $\frac{p}{2}$.

6- PRESENTION OF RESULT

In this section, the solution results to the self similar equations (30), (31) and (32) and the semi-similar equations (10) to (12) and (16) to (19) along with surface shear stresses for different functions of axial/angular velocities and prescribed values of wall temperature or wall heat flux. Entire solution is presented for different Reynolds and Prandtl numbers and different values of dimensionless transpiration rate, $S(t)$.

Figures (2)-(7) present the semi-similar solution for dimensionless transpiration rate, $S(t) = t + 1$, in which the function $F(h,t)$ is shown in terms of

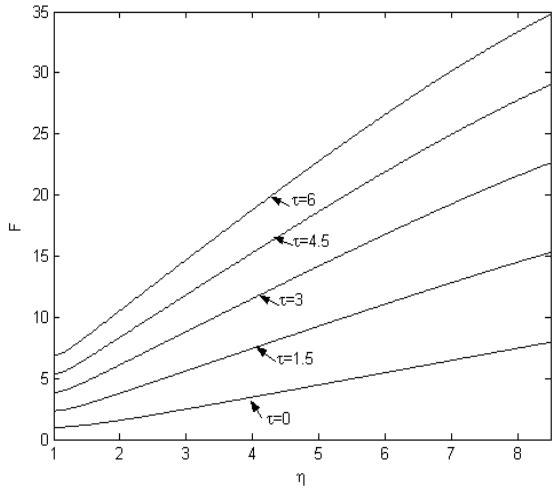

Figure 2. Sample profiles of $F(h,t)$ function for $S(t) = (t+1)$, for selected values of non-dimensional time at Re=1.

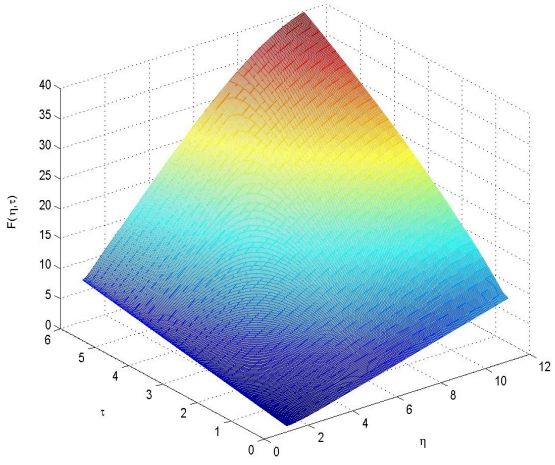

Figure 3. Surface function $F(h,t)$ for $s(t) = (t+1)$ $\mathrm{Re} = 1$.

h and for different non-dimensional time values at Re=1, 10, and 100. The process of obtaining this solution is explained in Sec.4. This function, for the first time, was solved by Wang [5] for the case of S=0 and later was presented by Cunning [11] for selected values
of suction rate. It is evident for this figure that, as non-dimensional time values increase, the F function increases, because of the dimensionless transpiration rate is an ascendant function of t . On the other hand, as

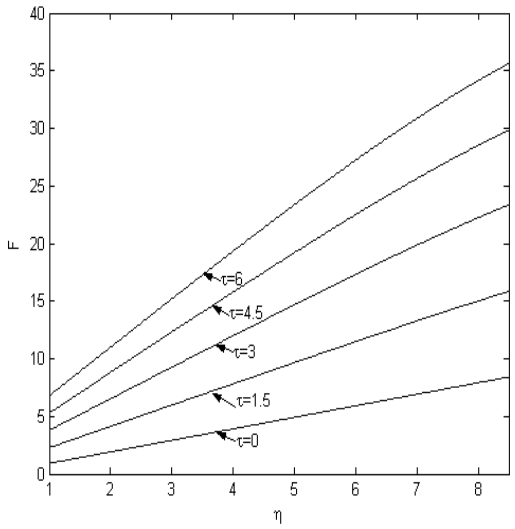

Figure 4. Sample profiles of $F(h,t)$ function for $S(t)=(t+1)$, for selected values of non-dimensional time at Re=10.

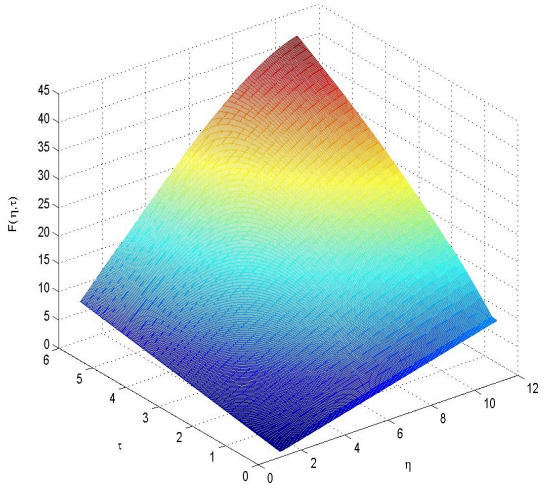

Figure 5. Surface function $F(h,t)$ for $s(t)=(t+1)$ $\mathrm{Re}=10$.

dimensionless transpiration increases, the F function increases and if $S(t)$ decreases, the F function decreases.

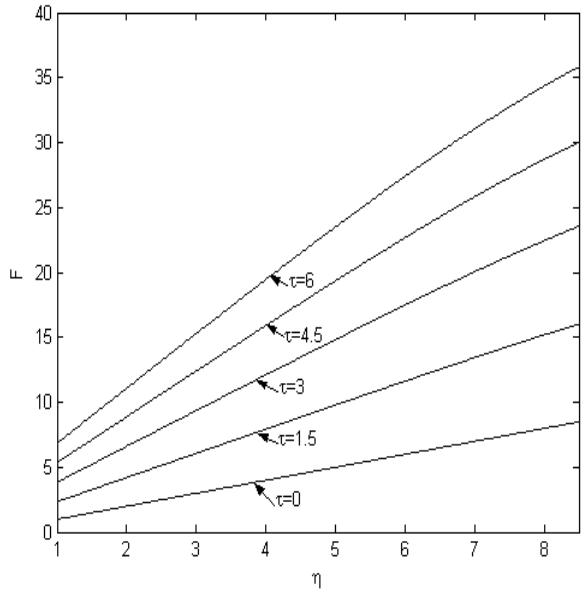

Figure 6. Sample profiles of $F(h,t)$ function for $S(t)=(t+1)$, for selected values of non-dimensional time at Re=100.

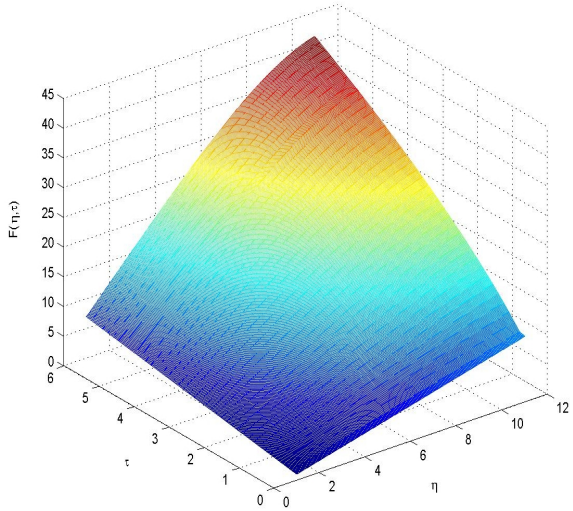

Figure 7. Surface function $F(h,t)$ for $s(t)=(t+1)$ $\mathrm{Re}=100$.

Figures (8)-(11) presents the same function but for the transpiration rate of $S(t) = (t+1)^{-1}$ and selected values of Reynolds numbers. Sample profiles of F'' function in terms of h are depicted in Figs (12) - (15) for different values of transpiration rates and selected values of Reynolds numbers. Figures (16) –

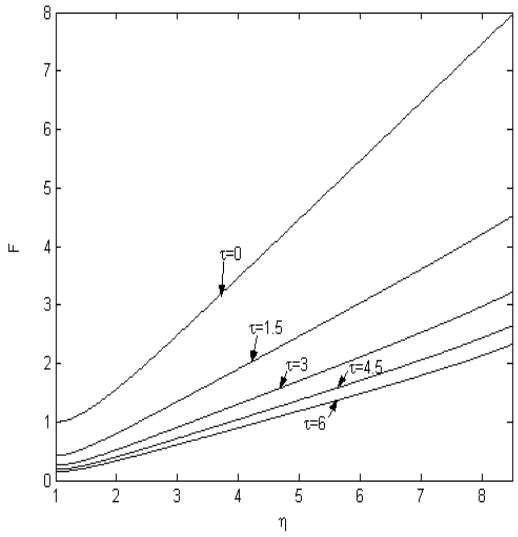

Figure 8. Sample profiles of $F(h,t)$ function for $s(t) = (t+1)^{-1}$ and selected values of non-dimensional time at Re=1.

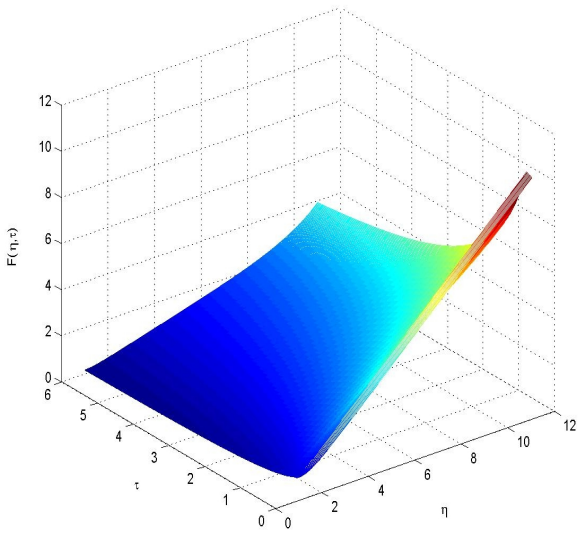

Figure 9. Surface function $F(h,t)$ for $s(t) = (t+1)^{-1}$ and $\mathrm{Re} = 1$

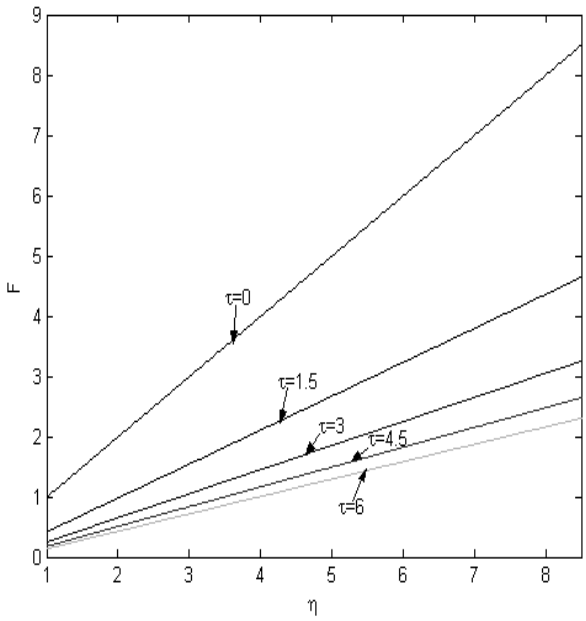

Figure 10. Sample profiles of $F(h,t)$ function for, for $s(t) = (t+1)^{-1}$ and selected values of non-dimensional
time at Re=100

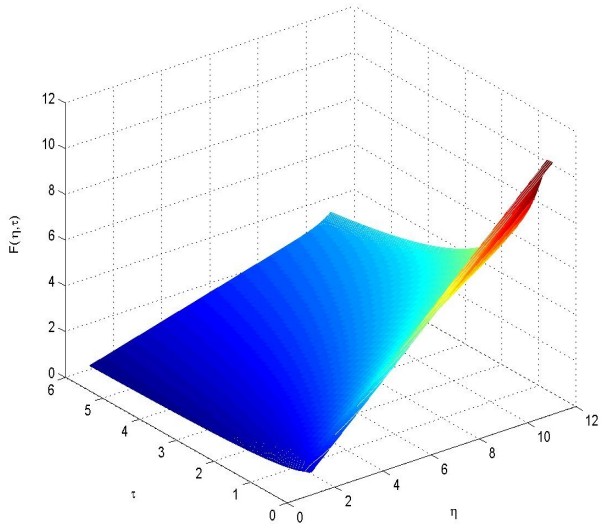

Figure 11. Surface function $F(h,t)$ for $s(t) = (t+1)^{-1}$ and $\mathrm{Re} = 100$

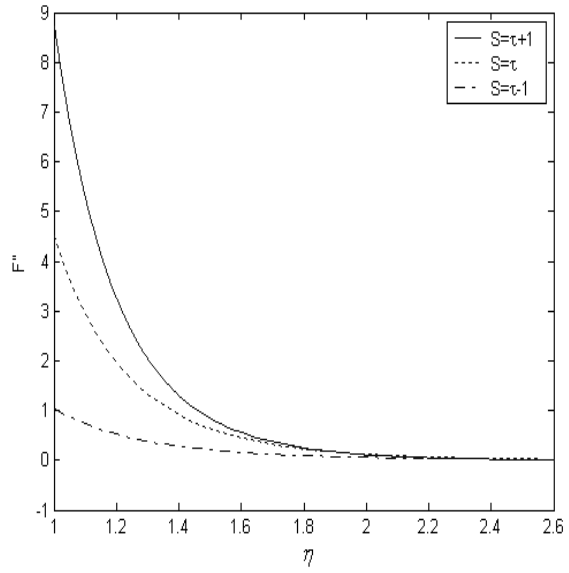

Figure 12. Sample profiles of F'' function for various function of dimensionless transpiration rate at Re=1 & $t = 1.5$.

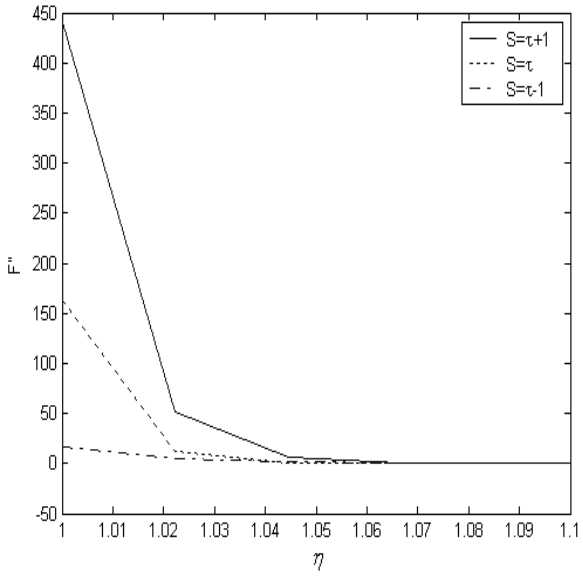

Figure 14. Sample profiles of F'' function for various function of dimensionless transpiration rate at Re=100 & $t = 1.5$.

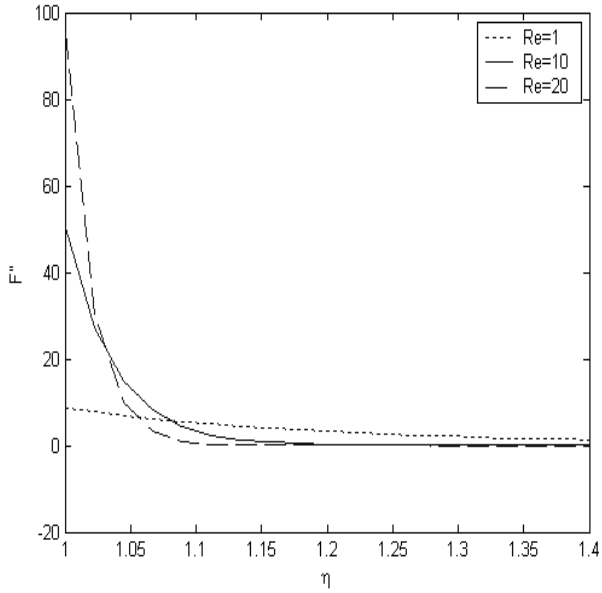

Figure 13. Sample profiles of F'' function at different Reynolds number for $S(t) = t + 1 \& t = 1.5$

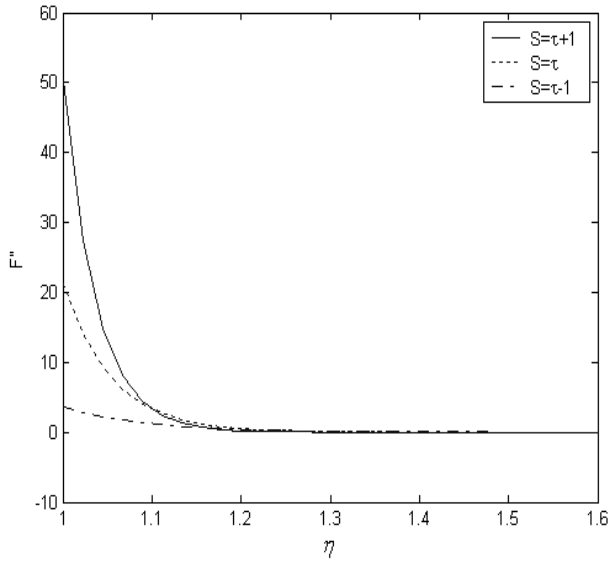

Figure 15. Sample profiles of F'' function for various function of dimensionless transpiration rate at Re=10 & $t = 1.5$

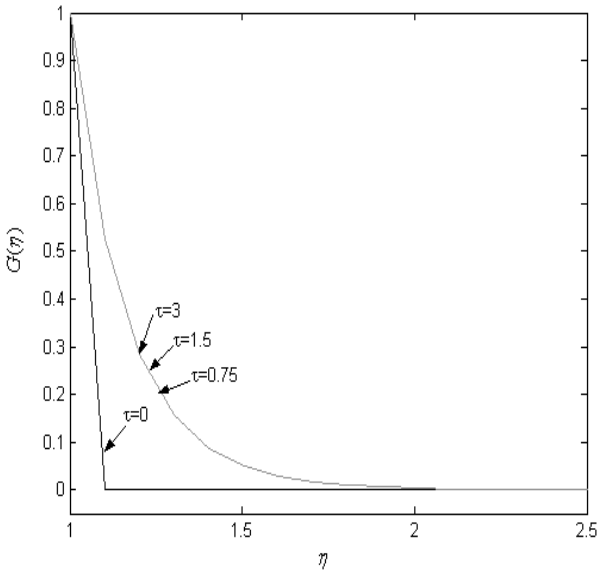

Figure 16. Sample profiles of $G(h,t)$ function for cylinder with angular velocity, $w(t)=1$, for selected values of non-dimensional time at Re=1, $S(t)=t+1$

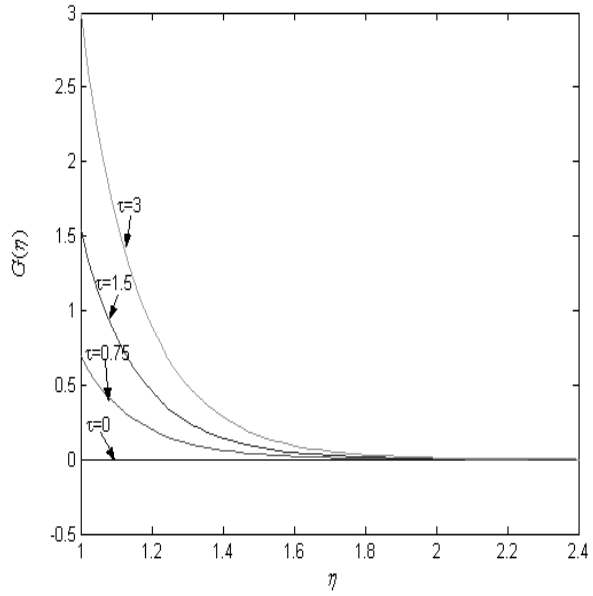

Figure 18. Sample profiles of $G(h,t)$ function for cylinder with angular velocity, $w(t)=t$, for selected values of non-dimensional time at Re=1.

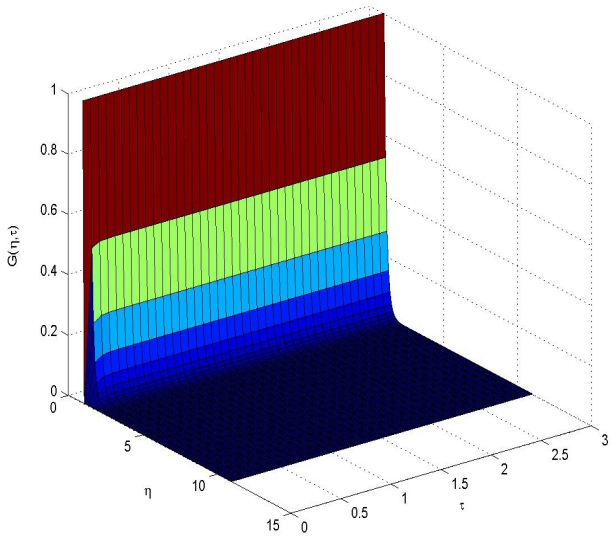

Figure 17- Function $G(h,t)$ in terms of h و t for circular function $w(t)=1$ and $\mathrm{Re}=1$

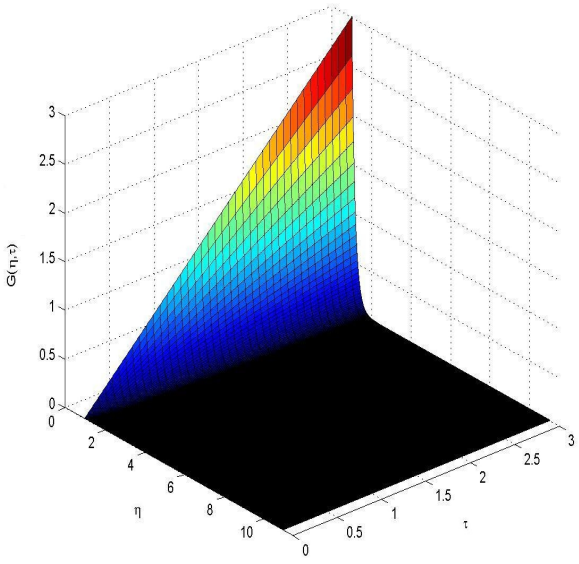

Figure 19. Function $G(h,t)$ in terms of h و t for circular function $w(t)=t$ and $\mathrm{Re}=1$

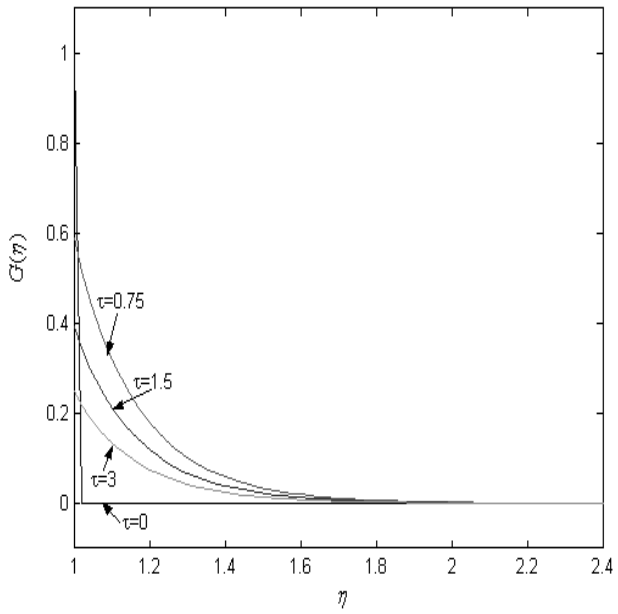

Figure 20. Sample profiles of $G(h,t)$ function for cylinder with angular velocity, $w(t)=(1+t)^{-1}$, for selected values of non-dimensional time at Re=1.

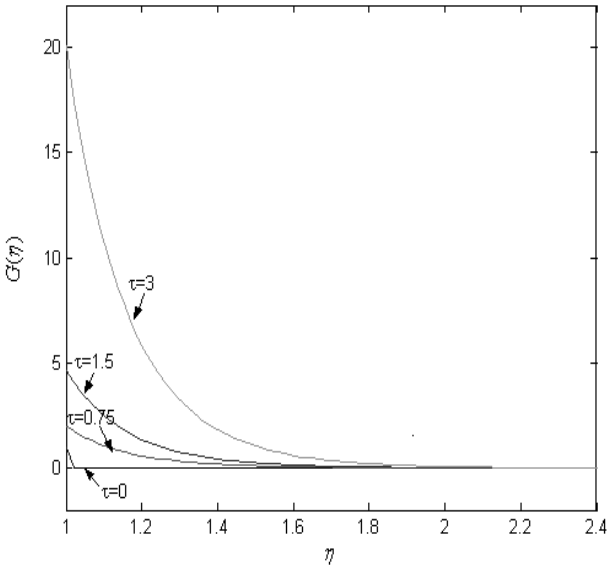

Figure 22 Sample profiles of $G(h,t)$ function for cylinder with angular velocity $w(t)=\exp(t)$, for selected values of non-dimensional time at Re=1.

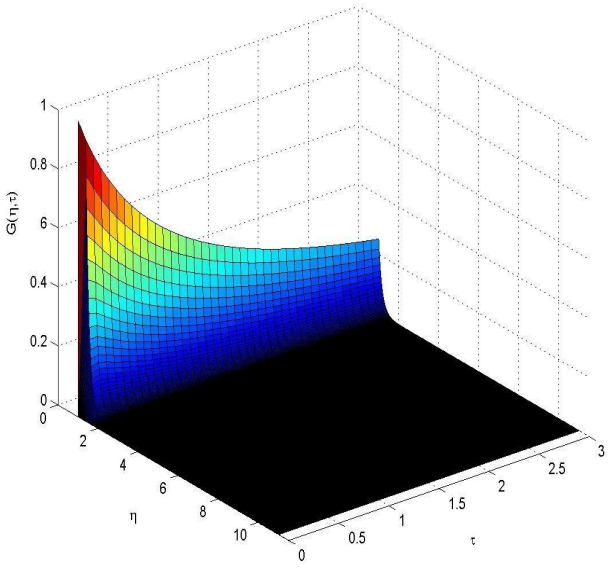

Figure 21. Function $G(h,t)$ in terms of h و t for circular function $w(t)=(1+t)^{-1}$ and $\mathrm{Re}=1$.

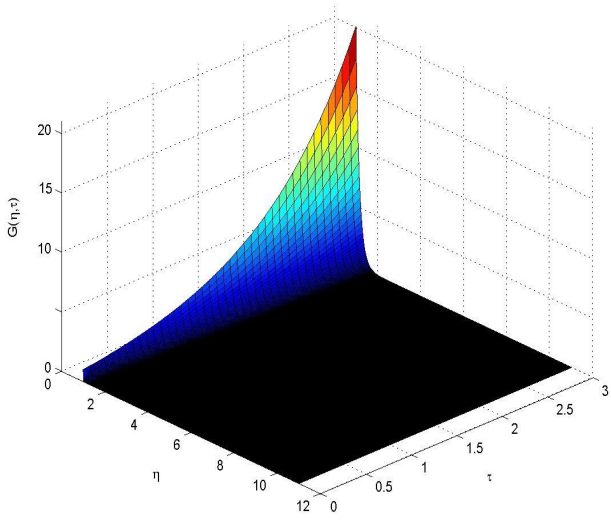

Figure 23. Function $G(h,t)$ in terms of h و t for circular function $w(t)=\exp(t)$ and $\mathrm{Re}=1$.

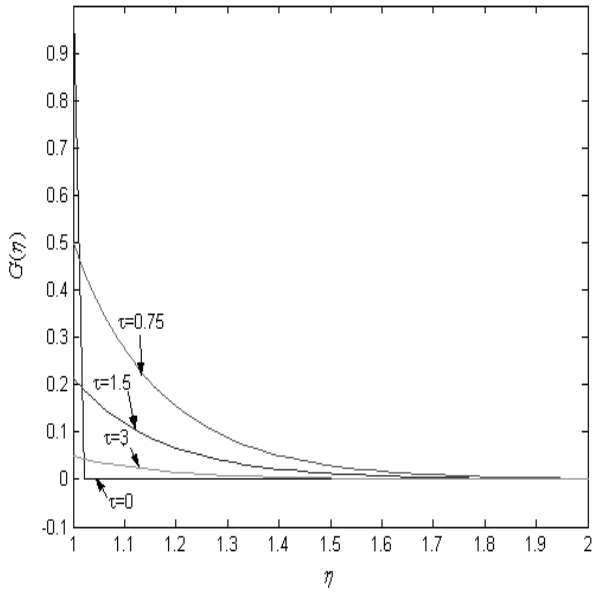

Figure 24. Sample profiles of $G(h,t)$ function for cylinder with angular velocity, $w(t)=\exp(-t)$, for selected values of non-dimensional time at Re=1.

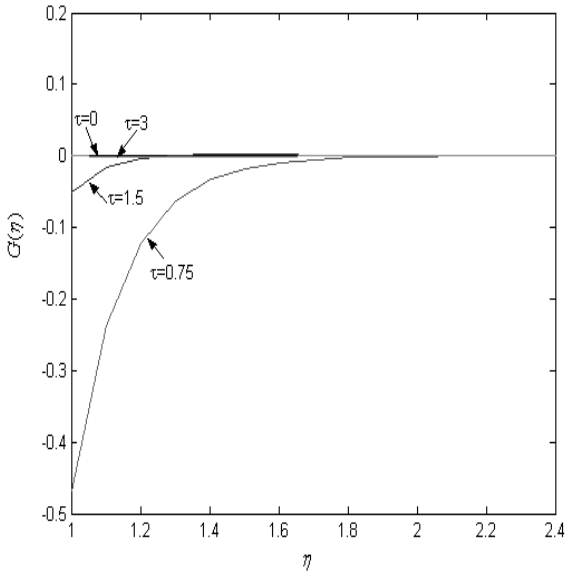

Figure 26. Sample profiles of $G(h,t)$ function for cylinder with angular velocity, $w(t)=\exp(-t).\sin(t)$, for selected values of non-dimensional time at Re=1.

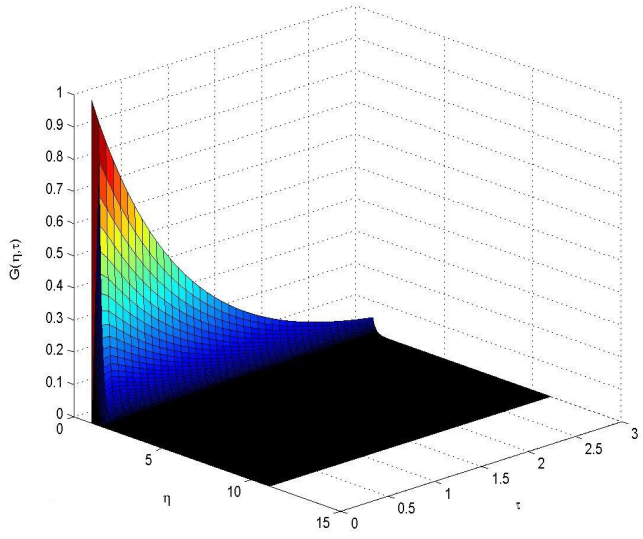

Figure 25. Function $G(h,t)$ in terms of h و t for circular function $w(t)=\exp(-t)$ and $\mathrm{Re}=1$.

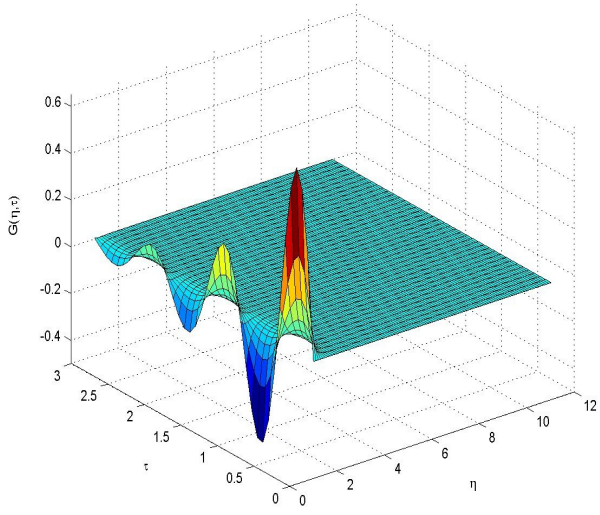

Figure 27 Function $G(h,t)$ in terms of h و t for circular function $w(t)=\exp(-t).\sin(t)$ and $\mathrm{Re}=1$.

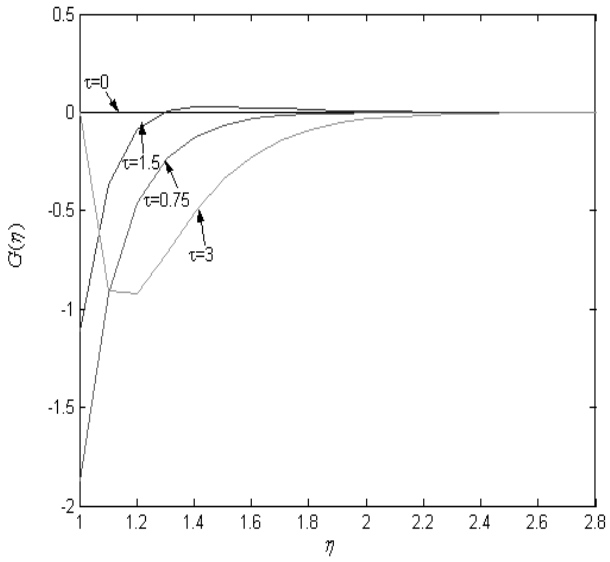

Figure 28. Sample profiles of $G(h,t)$ function for cylinder
with angular velocity $w(t) = \exp(t).\sin(t)$ for selected values of non-dimensional time at Re=1

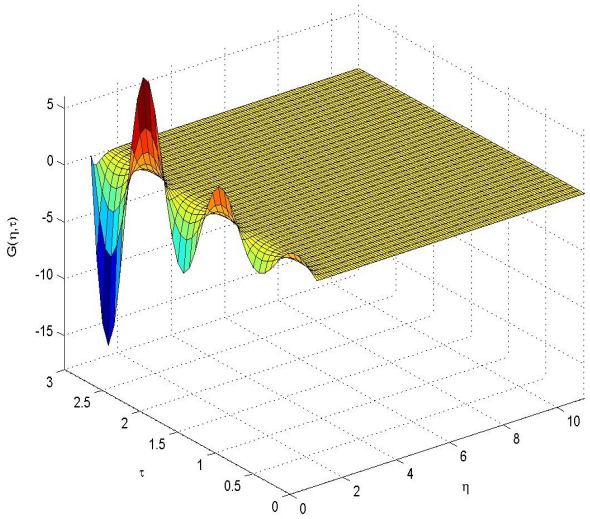

Figure 29. Function $G(h,t)$ in terms of h و t for circular function $w(t) = \exp(t).\sin(t)$ and $\mathrm{Re} = 1$.

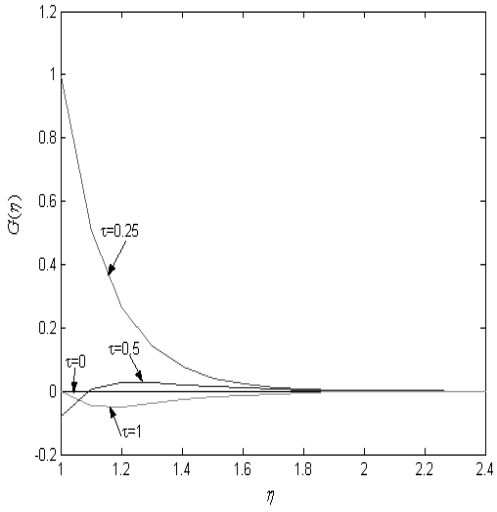

Figure 30. Sample profiles of $G(h,t)$ function for cylinder with angular velocity $w(t) = \sin(t)$ in terms of h for selected values of non-dimensional time at Re=1.

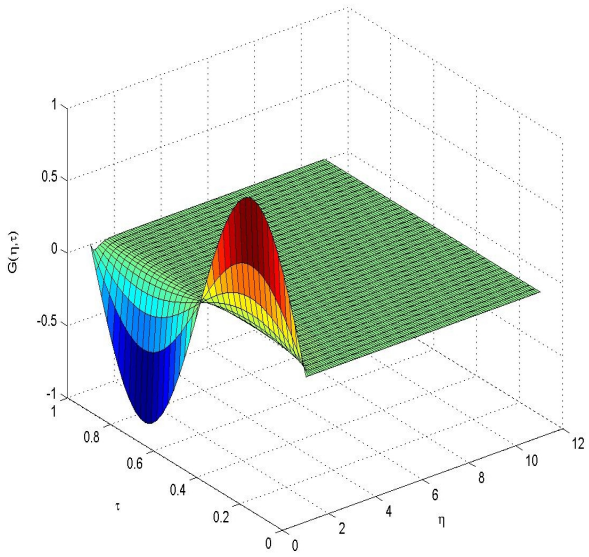

Figure 31. Function $G(h,t)$ in terms of h و t for circular function $w(t) = \sin(t)$ and $\mathrm{Re} = 1$.

(31) present the function $G(h,t)$ for cylinder with selected values of angular velocity along with its corresponding surface function for different values of non-dimensional time at Re=1, and transpiration rate

of $S(t)=t+1$. Different situations occur which are depicted in the diagrams.

Figures (32) to (41) show sample profiles of $H(h,t)$ function for cylinder with selected values of axial velocity in terms of h and for different values of non-dimensional time at Re=1and for transpiration rate of $S(t)=t+1$. Different situations can be observed in these diagrams depending on the different factors.

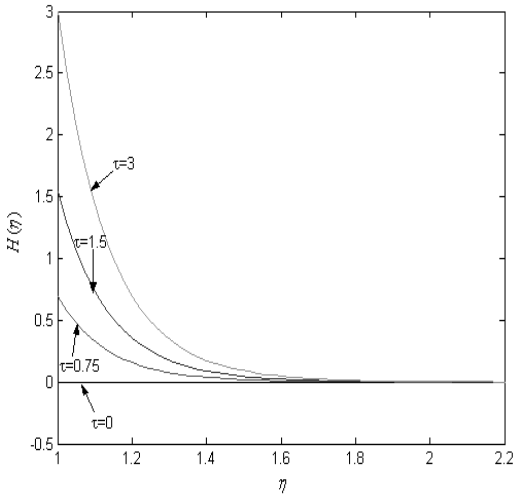

Figure 32. Sample profiles of $H(h,t)$ function for cylinder with axial velocity, $V(t)=t$, in terms of h and for selected values of non-dimensional time at Re=1, $S(t)=t+1$.

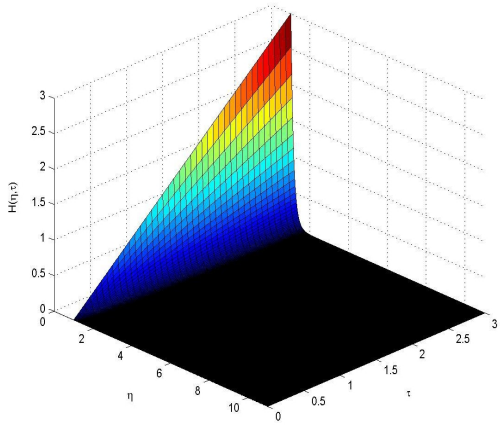

Figure 33. Function $H(h,t)$ in terms of h ، t for axial velocity $V(t)=t$ and $\mathrm{Re}=1$

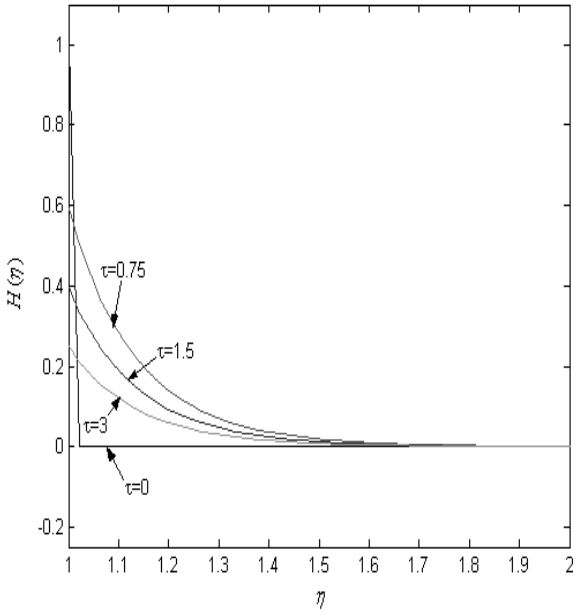

Figure 34. Sample profiles of $H(h,t)$ function for cylinder with axial velocity, $V(t)=(1+t)^{-1}$, in terms of h and for selected values of non-dimensional time at Re=1.

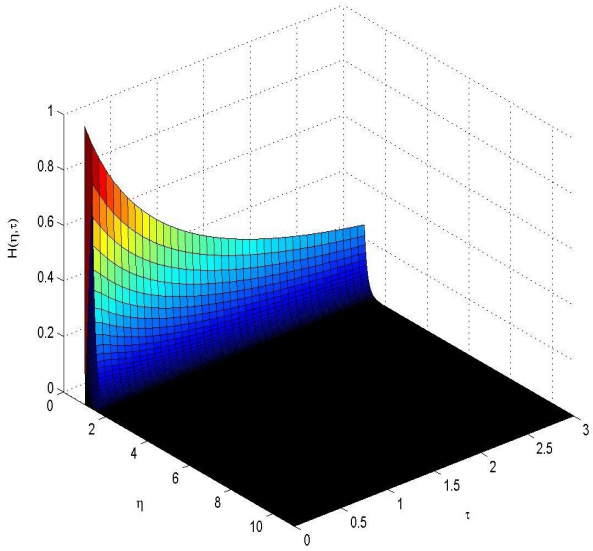

Figure 35. Function $H(h,t)$ in terms of h ، t axial velocity $V(t)=(1+t)^{-1}$ and $\mathrm{Re}=1$

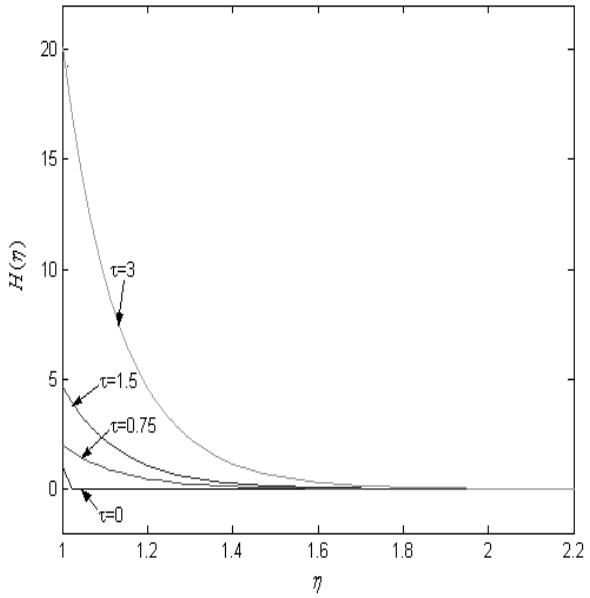

Figure 36 Sample profiles of $H(h,t)$ function for cylinder bwith axial velocity, $V(t)=\exp(t)$, in terms of h and for selected values of non-dimensional time at Re=1.

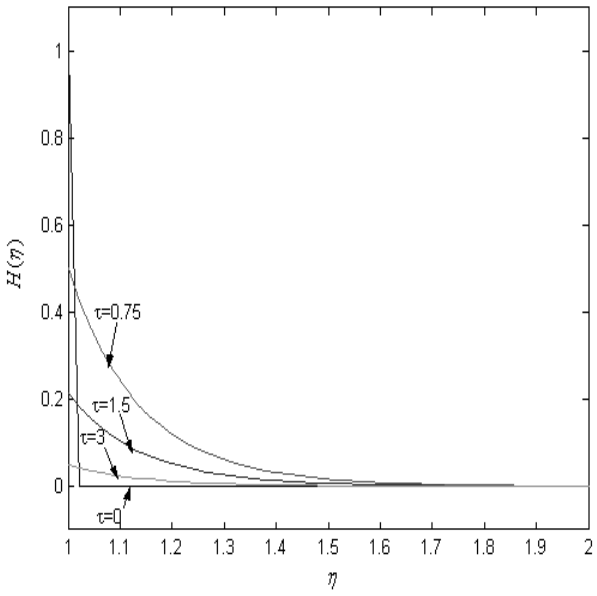

Figure 38. Sample profiles of $H(h,t)$ function for cylinder with axial velocity, $V(t)=\exp(-t)$, in terms of h and for selected values of non-dimensional time at Re=1

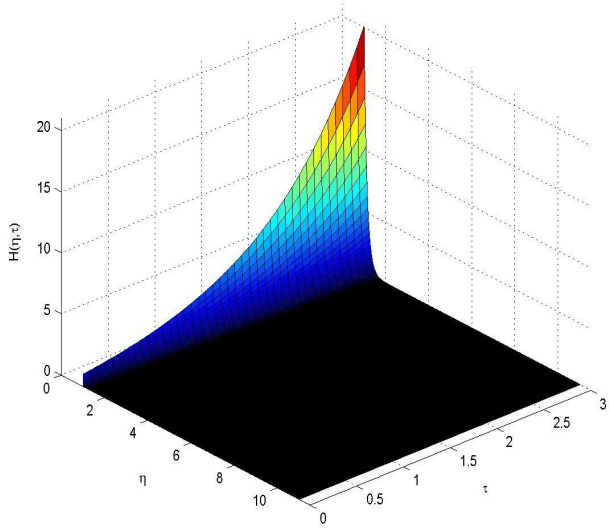

Figure 37. Function $H(h,t)$ in terms of h , t for axial velocity $V(t)=\exp(t)$ $\mathrm{Re}=1$

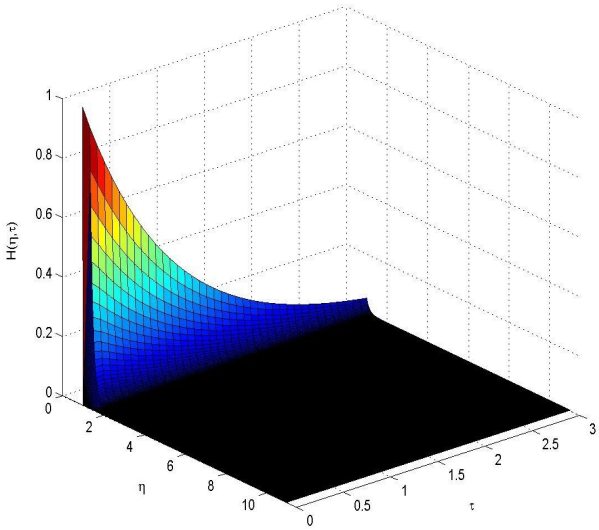

Figure 39. Function $H(h,t)$ in terms of h , t and for axial velocity $V(t)=\exp(-t)$ and $\mathrm{Re}=1$

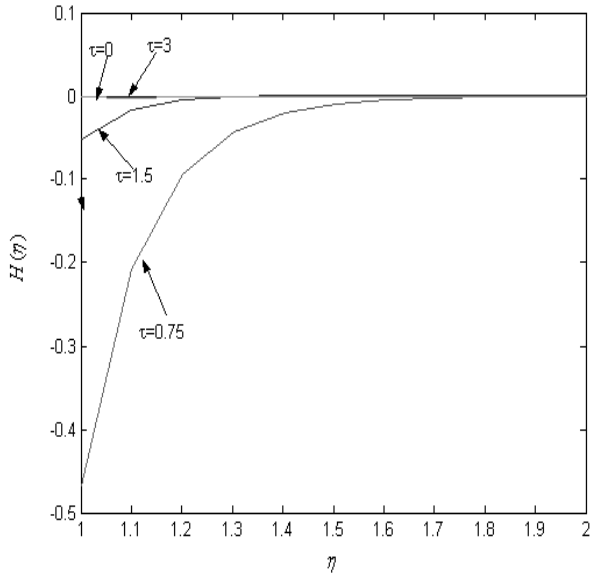

Figure 40. Sample profiles of $H(h,t)$ function for cylinder with axial velocity, $V(t)=\exp(-t).\sin(t)$ in terms of h and for selected values of non dimensional time at Re=1.

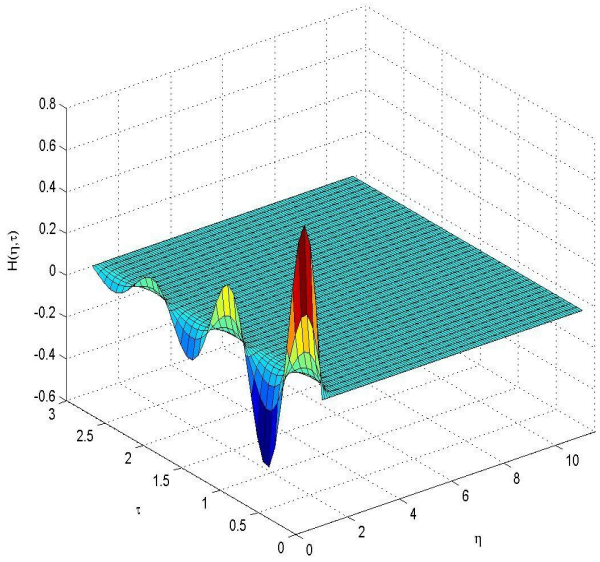

Figure 41. Function $H(h,t)$ in terms of h , t for axial velocity $V(t)=\exp(-t).\sin(t)$ and $\mathrm{Re}=1$.

Figures (42) to (53) present the effect of transpiration on tangential shear stress for the cylinder rotating with selected angular velocity and for different values of transpiration rate along with different values of Reynolds numbers.

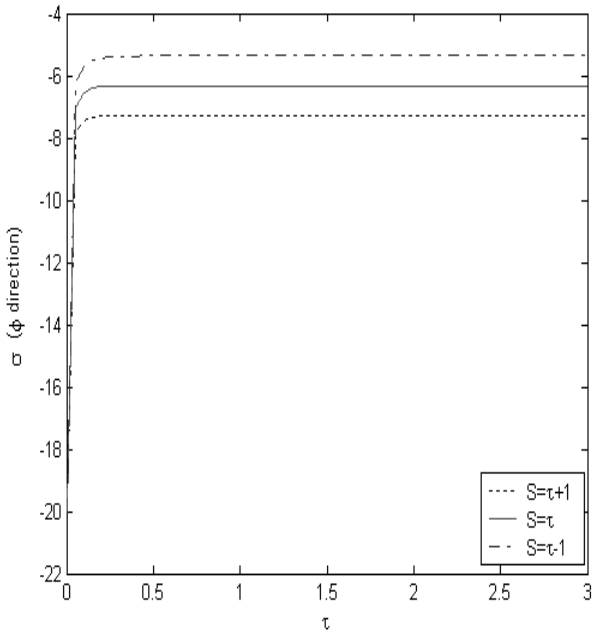

Figure 42. Effect of transpiration on tangential shear stress for cylinder rotation with $w(t)=1$

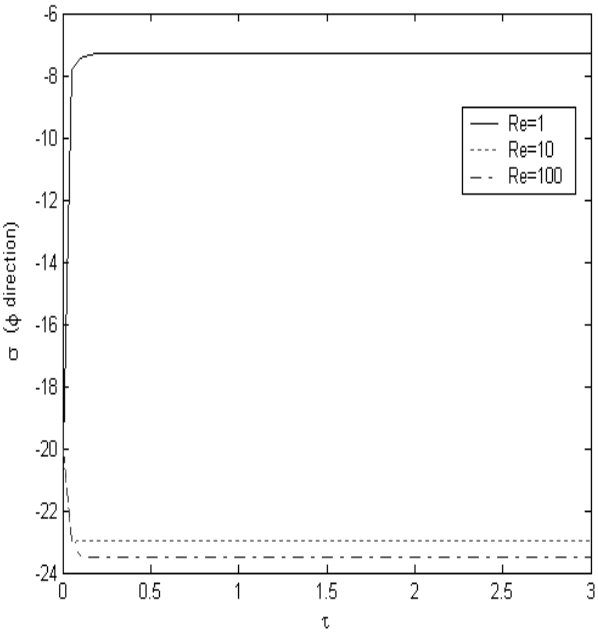

Figure 43. Effect of Reynolds number on tangential shearstress for cylinder rotation with $w(t)=1$

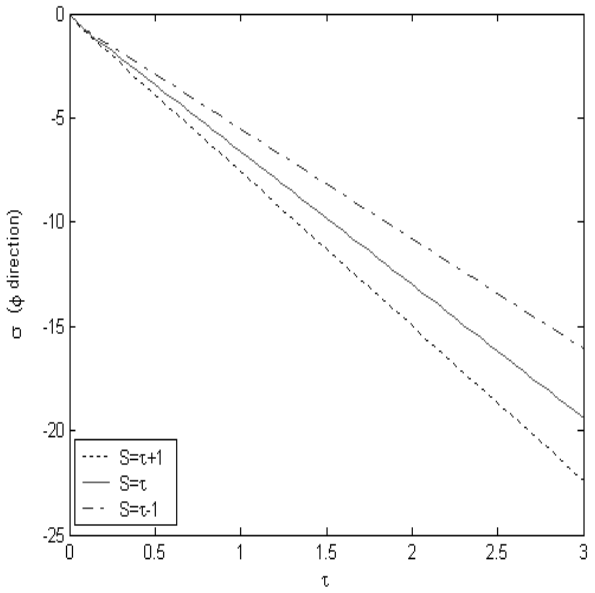

Figure 44. Effect of transpiration on tangential shear stress for cylinder rotation with $w(t) = t$

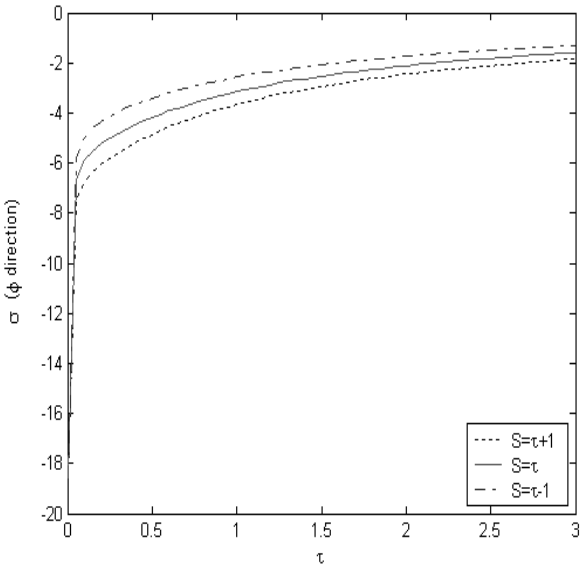

Fig.ure 46. Effect of transpiration on tangential shear stress for cylinder rotation with $w(t) = (t+1)^{-1}$

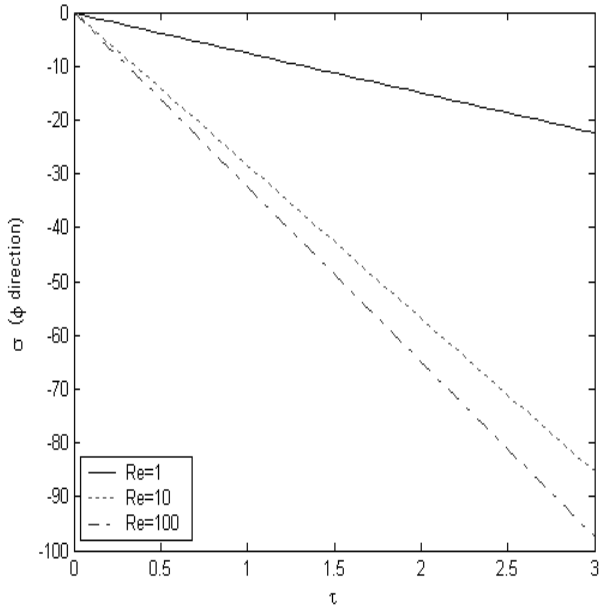

Figure 45. Effect of Reynolds number on tangential shear stress for cylinder rotation with $w(t) = t$

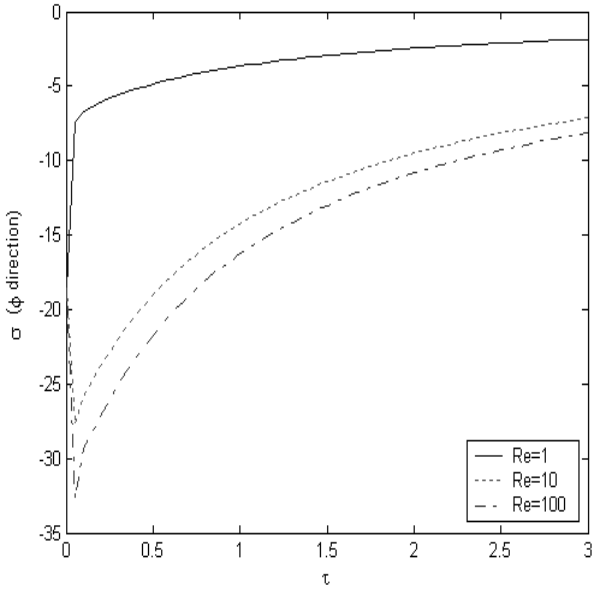

Figure 47. Effect of Reynolds number on tangential shear stress for cylinder rotation with $w(t) = t$ $w(t) = (t+1)^{-1}$

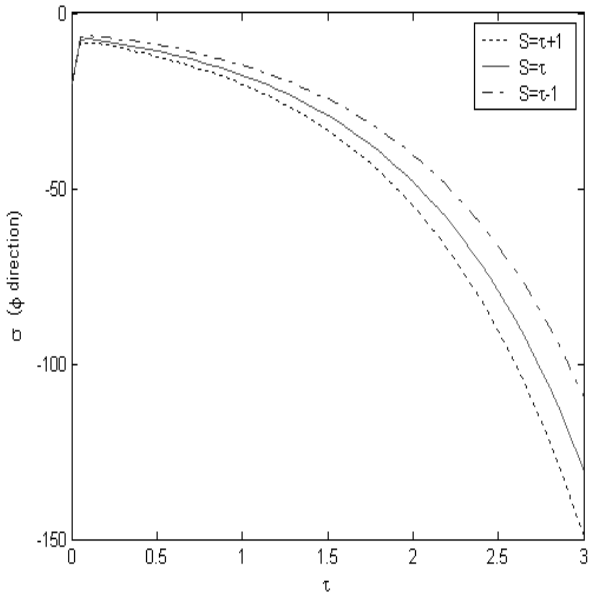

Figure 48. Effect of transpiration on tangential shear stress for cylinder rotation with $w(t) = \exp(t)$

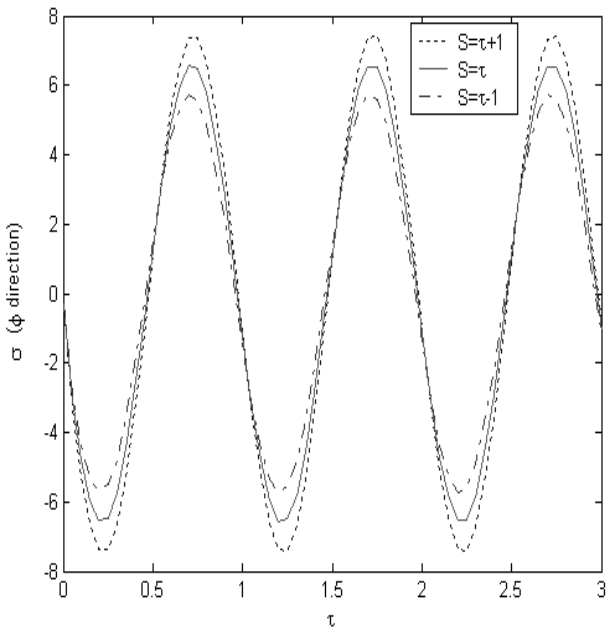

Figure 50. Effect of transpiration on tangential shear stress for cylinder rotation with $w(t) = \sin(t)$

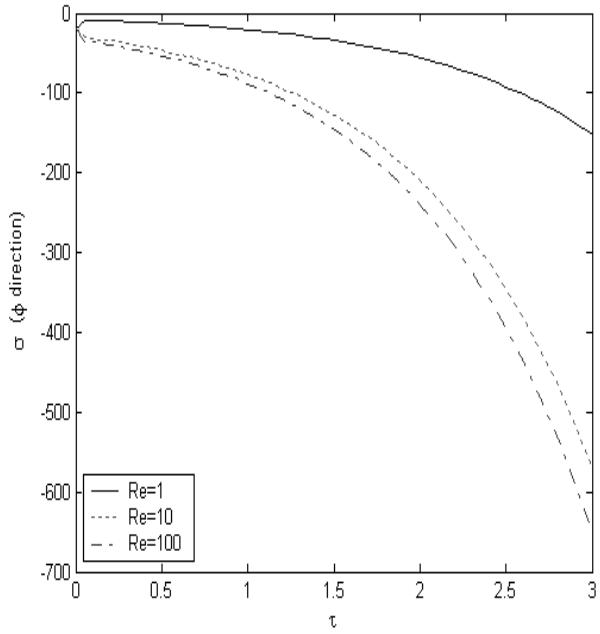

Figure 49. Effect of Reynolds number on tangential shear stress for cylinder rotation with $w(t) = \exp(t)$

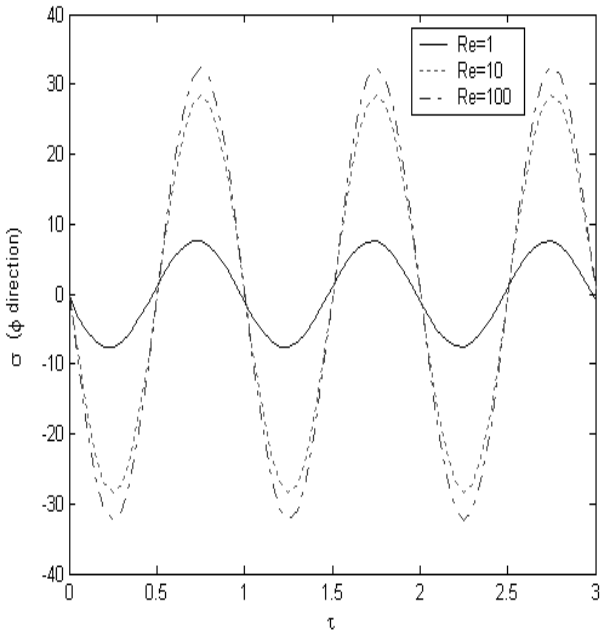

Figure 51. Effect of Reynolds number on tangential shear stress for cylinder rotation with $w(t) = \sin(t)$

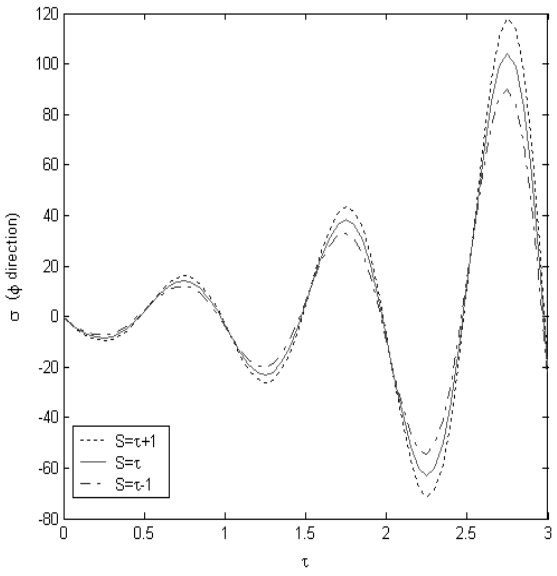

Figure 52. Effect of transpiration on tangential shear stress for cylinder rotation with $w(t) = \exp(t).\sin(t)$

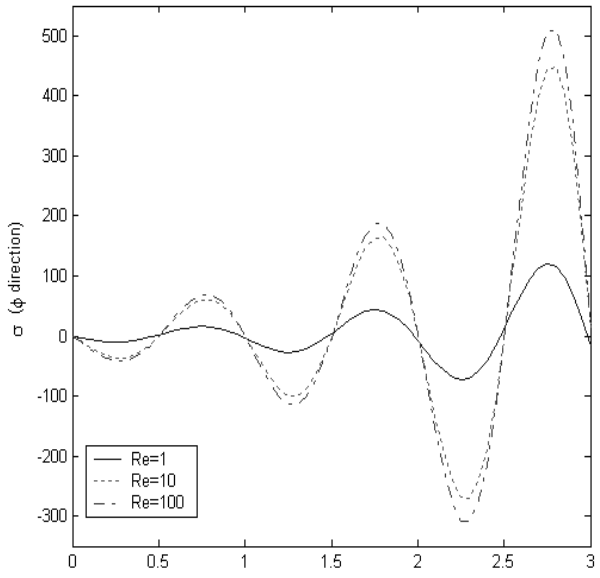

Figure 53. Effect of Reynolds number on tangential shear stress for cylinder rotation with $w(t) = \exp(t).\sin(t)$

Figures (54) to (67) show the effect of transpiration rate on axial shear stress for the cylinder moving in selected values of axial velocity and different values of Reynolds numbers. Finally, Figures (68) to (70) depict $\Theta(h,t)$ function for selected values of transpiration rate and different temperature functions. So in cooling process, high Prandtl number and Reynolds number fluid are preferred. Also, higher suction rates provide a means for cooling surface and higher blowing rates provide a means for heating the surface of the cylinder. Therefore in a defined wall heat flux case, to prevent high wall temperature, higher rates of suction can be provided and vice-versa.

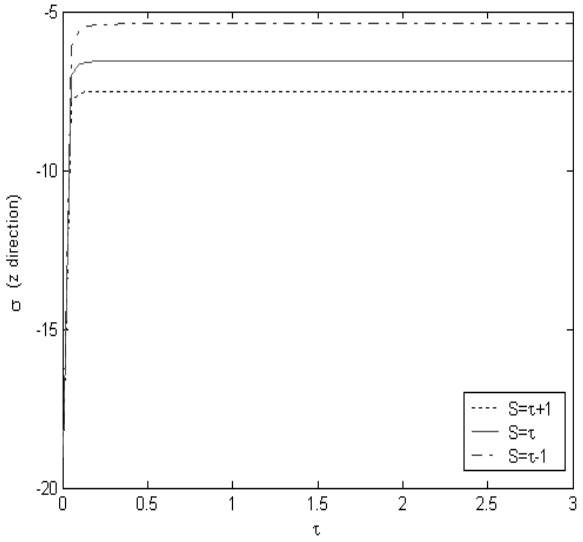

Figure 54. Effect of transpiration on axial shear stress for cylinder axial velocity of $V(t) = 1$

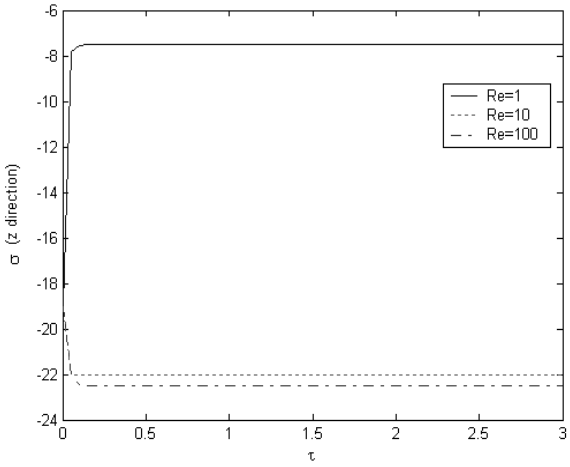

Figure 55. Effect of Reynolds number on axial shear stress for cylinder axial velocity of $V(t) = 1$

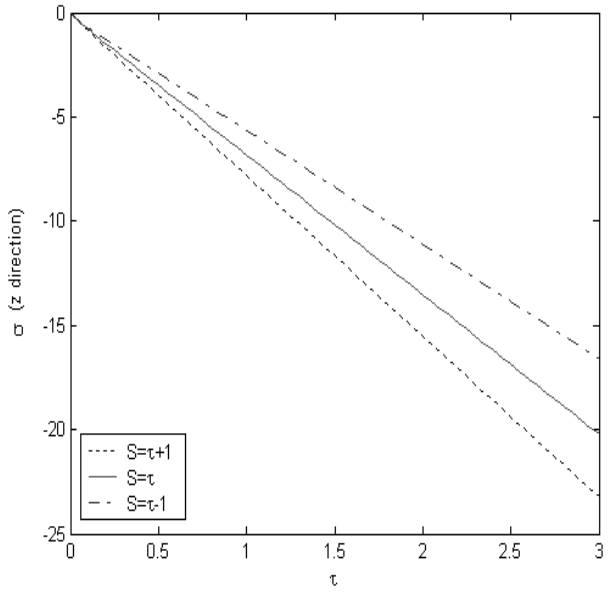

Figure 56. Effect of transpiration on axial shear stress for cylinder axial velocity of $V(t) = t$

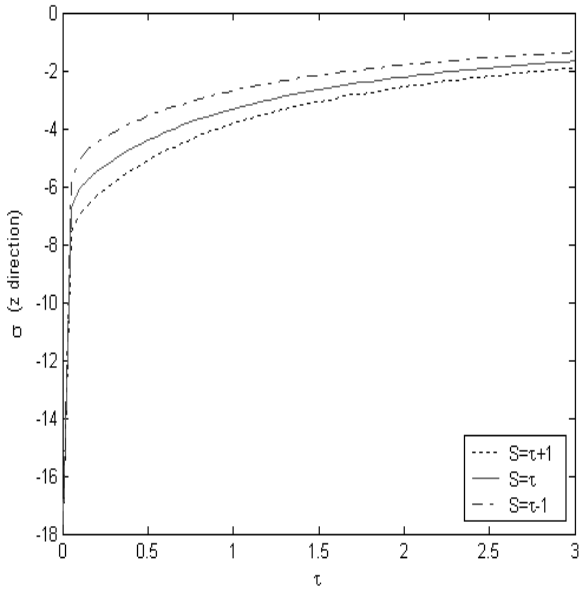

Figure 58. Effect of transpiration on axial shear stress for cylinder axial velocity of $V(t) = (t+1)^{-1}$

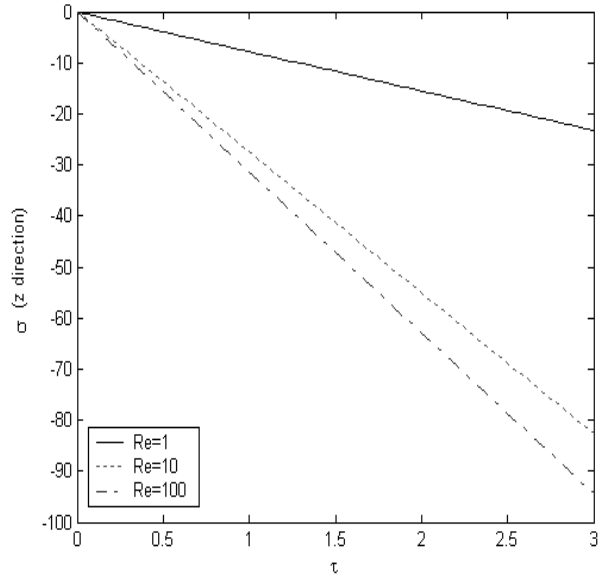

Figure 57. Effect of Reynolds number on axial shear stress for cylinder axial velocity of $V(t) = t$

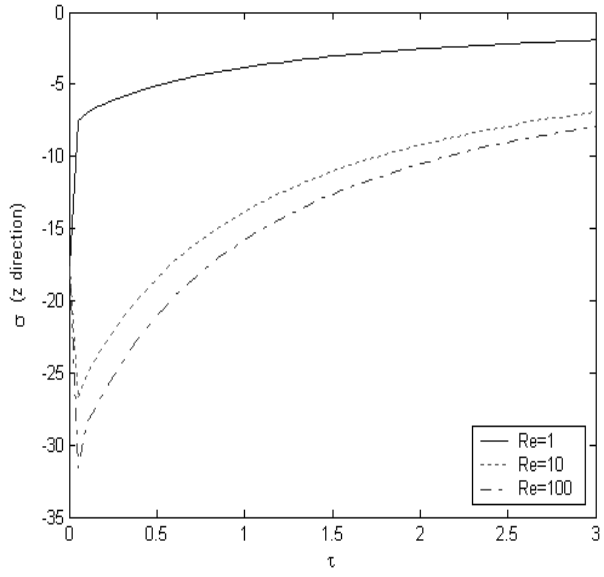

Figure 59. Effect of Reynolds number on axial shear stress for cylinder axial velocity of $V(t) = (t+1)^{-1}$

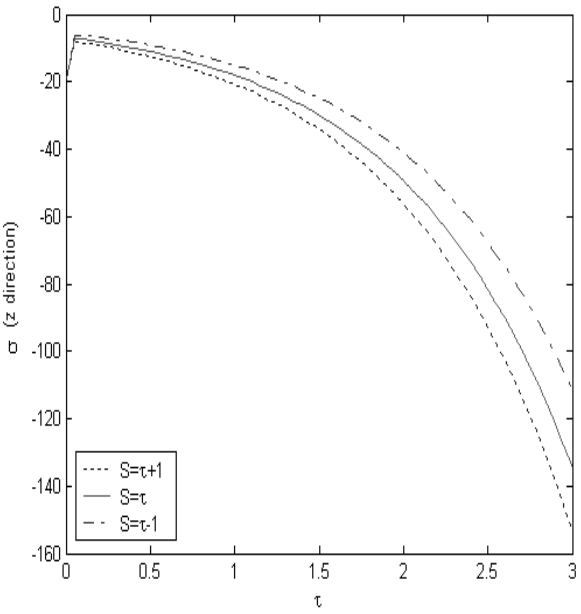

Figure 60. Effect of transpiration on axial shear stress for cylinder axial velocity of $V(t) = \exp(t)$

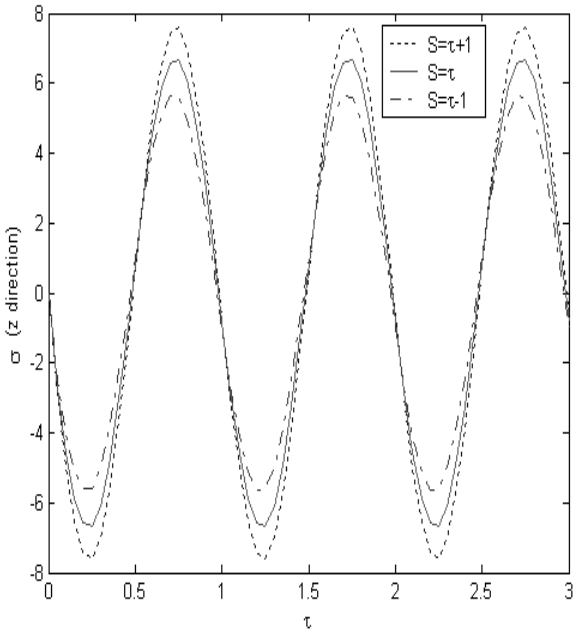

Figure 62. Effect of transpiration on axial shear stress for cylinder axial velocity of $V(t) = \sin(t)$

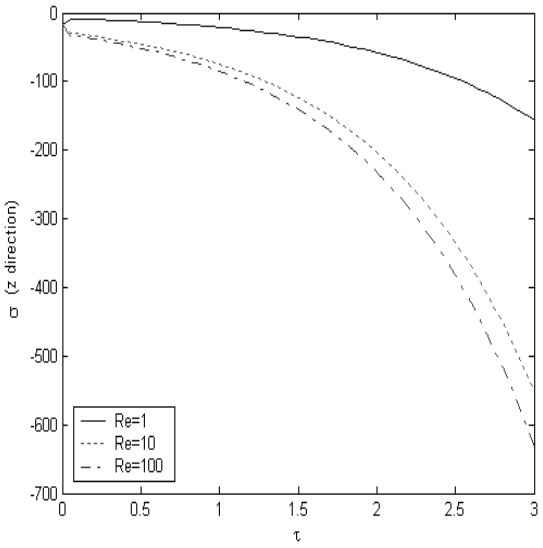

Figure 61. Effect of Reynolds number on axial shear stress for cylinder axial velocity of $V(t) = \exp(t)$

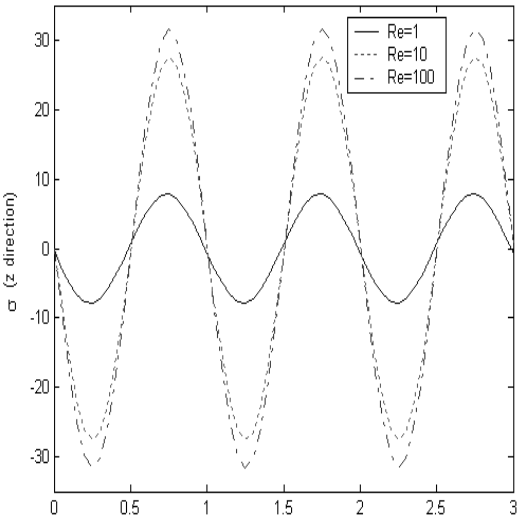

Figure 63. Effect of Reynolds number on axial shear stress for cylinder axial velocity of $V(t) = \sin(t)$

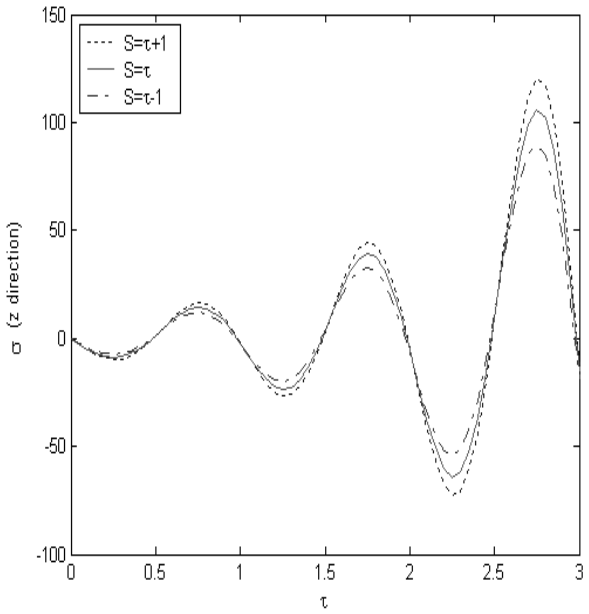

Figure 64. Effect of transpiration on axial shear stress for cylinder axial velocity $V(t) = \exp(t).\sin(t)$

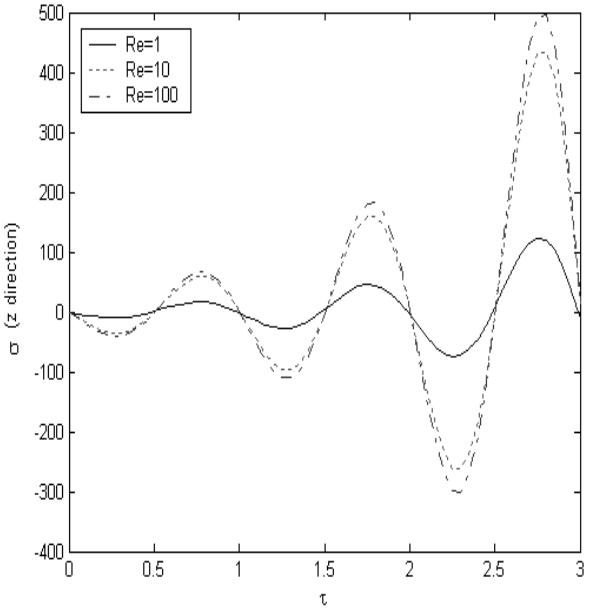

Figure 65. Effect of Reynolds number on axial shear stress for cylinder axial velocity of $V(t) = \exp(t).\sin(t)$

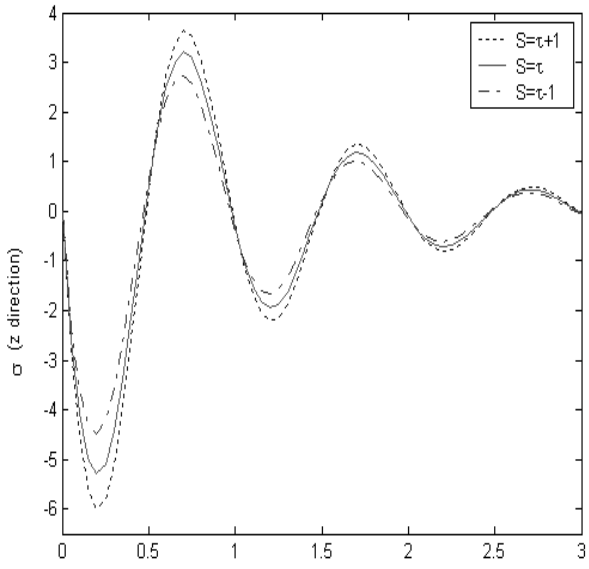

Figure 66. Effect of transpiration on axial shear stress for cylinder axial velocity $V(t) = \exp(-t).\sin(t)$

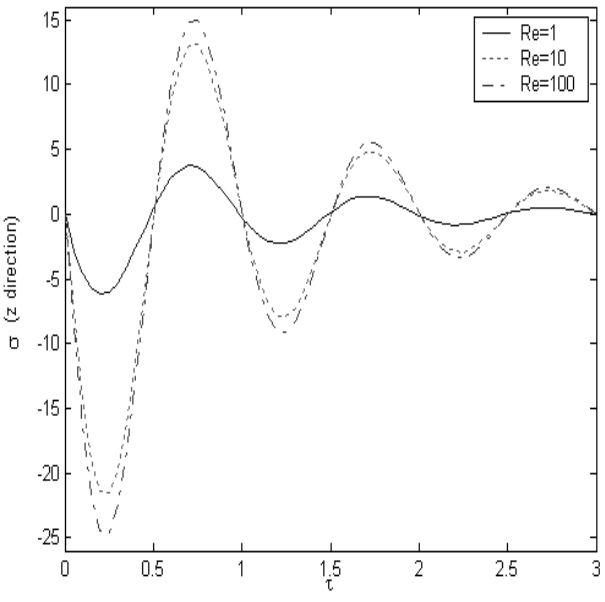

Figure 67. Effect of Reynolds number on axial shear stress for cylinder axial velocity of $V(t) = \exp(-t).\sin(t)$

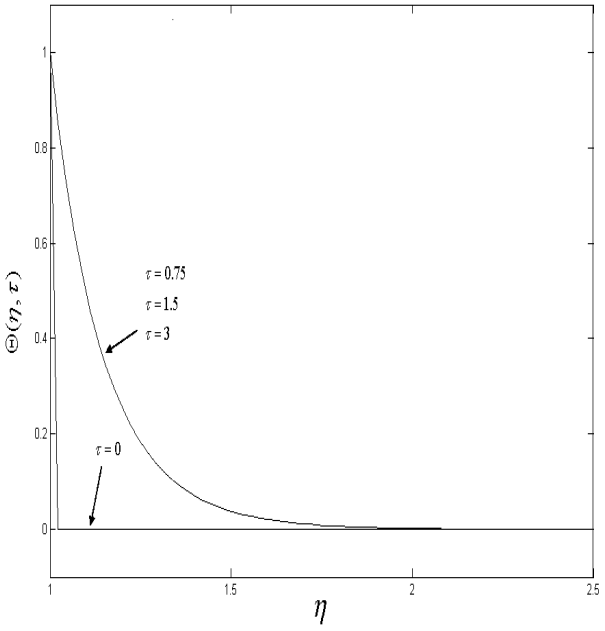

Figure 68. $\Theta(h,t)$ function for $S(t) = t + 1$ and the case of $T - T_w = \text{constant}$

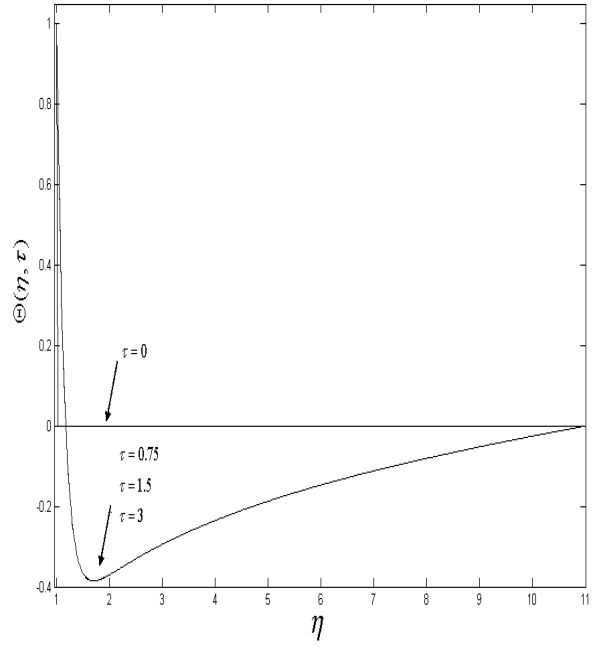

Figure 69. $\Theta(h,t)$ function for $S(t) = (t+1)^{-1}$ and the case of $T - T_w = Exp(t)$

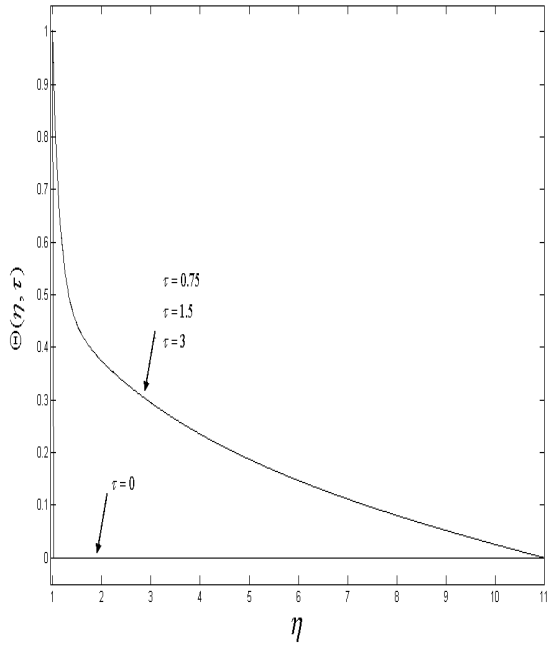

Figure 70. $\Theta(h,t)$ function for $S(t) = \cos t$ and the case of $T - T_w = Exp(-t)$.

6. CONCLUTION

A numerical solution of the Navier-Stokes equations and energy equation is obtained for the problem of stagnation–point flow on a circular cylinder with time-dependent normal transpiration. A general semi-similar solution is obtained when cylinder has different forms of axial/rotational motions including: constant axial/angular velocity, exponential axial/angular velocity, pure harmonic movement/rotation, both accelerating and decelerating oscillatory motion. Since the heat transfer is axisymmetric in the q direction, the cylinder rotation has no effect on temperature field. Results for different time-dependent wall temperature and heat flux functions including: constant wall temperature or heat flux, exponential and oscillatory form of wall temperature or wall heat flux are presented. Axial and azimuthal component of fluid velocity and surface axial and azimuthal shear stress on the cylinder are obtained in all above situations, and for different values of

Reynolds numbers and time-dependent transpiration.

Absolute value of axial /azimuthal shear stresses corresponding to all cases increase with the increase Reynolds number and suction rate. In defined wall temperature case, heat transfer increases with the increase of Reynolds number, Prandtl number and suction rate, where as the depth of the diffusion of temperature field decreases. So, an increase of suction rate can be used as means of cooling the surface and increase if blowing can be used as a means of heating surface. It is shown that by providing blowing on the surface of a cylinder, reduction of resistance against its axial/rotational movement inside a fluid can be achieved. It is also found that higher suction rates are means for cooling the surface and higher blowing rates are a means of heating the surface of cylinder.

7. REFRENCES

1. Hiemenz, K., "Die Grenzchicht an einem in den gleichformingen Flussigkeitsstrom eingetauchten graden Kreiszylinder," ***Dinglers Polytech. J.***, Vol. 236, (1911), 321-410.
2. Homann, F.Z., "Der Einfluss grosser Zahighkeit bei der Strmung um den Zylinder und um die Kugel," ***Zeitsch. Angew. Math. Mech.***, Vol. 16, (1936), 153-164.
3. Howarth, L., "The boundary layer in three dimensional flow," Part II. "The flow near a stagnation point," ***Phill. Mag. Series*** 7, Vol. 42, (1951), 1433-1440.
4. Davey, A., "Boundary layer flow at a saddle point of attachment," ***Journal of Fluid Mechanics***, Vol. 10, (1951), 593-610.
5. Wang, C., "Axisymmetric stagnation flow on a cylinder," ***Quaterly of applied Mathematics***, Vol. 10, (1974), 207-213.
6. Gorla, R.S.R., "Heat transfer in axisymmetric stagnation flow on a cylinder," ***Applied Scientific Research J.***, Vol.32, November (1976), 541-553.
7. Gorla, R.S.R., "Unsteady laminar axisymmetric stagnation flow over a cylinder," ***Dev. Mech.***, Vol. 9 (1977), 286-288.
8. Gorla, R.S.R., "Non-similar axisymmetric stagnation flow on a moving cylinder," ***Int. J. Engineering Science***, Vol. 16, (1978), 392-400.
9. Gorla, R.S.R., "Transient response behavior of an axisymmetric stagnation flow on a circular cylinder due to time dependent free stream velocity," ***Lett. Appl. Eng. Sci.***, Vol. 16, (1978), 493-502.
10. Gorla, R.S.R., "Unsteady viscous flow in the vicinity of an axisymmetric stagnation point on a cylinder," ***Int. J. Engineering Science***, Vol. 17, (1979), 87-93.
11. Cunning, G.M., Davis, A.M.J., and Weidman, P.D., "Radial stagnation flow 0on a rotating cylinder with uniform transpiration," ***Journal of Engineering Mathematics***, Vol. 33, (1998),pp.113-128.
12. Takhar, H.S., Chamkha, A.J., and Nath, G., "unsteady axisymmetric stagnation point flow of a viscous fluid on a cylinder," ***Int. Journal of Engineering Science***, Vol. 37, (1999), 1943-1957.
13. Rahimi, A.B., "Heat transfer in an axisymmetric stagnation flow on a cylinder at high prandtl numbers using perturbation techniques," ***International Journal of Engineering Science***, Vol. 10(1) (1999), 37-57
14. Saleh, R., and Rahimi, A.B., "Axisymmetric stagnation point flow of a viscous fluid on a moving cylinder with time dependent axial velocity," ***International Journal of engineering***, Vol. 17, No.1, (2004), 99-108.
15. Saleh, R., and Rahimi, A.B., "Axisymmetric radial stagnation point flow of a viscous fluid on a rotating cylinder with time dependent axial angular velocity," ***Int. J. of Science and Technology***, Vol. 12, No.4, (fall 2005).
16. Saleh, R., and Rahimi, A.B., "Stagnation flow and heat transfer on a moving cylinder with transpiration and high Reynolds number consideration," ***Journal of Science and Technology***, Transaction B, Vol.28, No. B4, (2004).
17. Saleh, R., and Rahimi, A.B., "Axisymmetric stagnation point flow and heat transfer of a viscous fluid on a moving cylinder with time dependent axial velocity and uniform transpiration," ***Journal of Fluid Engineering-transaction of ASME***, Vol. 126, No.5, (November 2004), 67-82.
18. Rahimi, A.B., and Saleh, R., "Axisymmetric stagnation point flow and heat transfer of a viscous fluid on a rotating cylinder with time dependent angular velocity," ***Journal of fluids engineering***, (2007).
19. Rahimi, A.B., Saleh, R., "Unaxisymmetric heat transfer in Axisymmetric stagnation point flow of a viscous fluid on cylinder with simultaneous axial and rotational movement along with transpiration", ***Journal of Heat Transfer, Transaction of ASME***, (Oct 2007)
20. Press, W.H., Flannery, B.P., Teukolsky, S.A. and Vetterling, W.T., Numerical Recipes, The Art of Scientific Computing, Cambridge University Press, Cambridge, (1997).